Published for SISSA by Springer

Received: June 4, 2024
Accepted: September 23, 2024
Published: October 11, 2024

Search for a resonance decaying into a scalar particle and a Higgs boson in final states with leptons and two photons in proton-proton collisions at $\sqrt{s} = 13$ TeV with the ATLAS detector

The ATLAS collaboration

E-mail: atlas.publications@cern.ch

Abstract: A search for a hypothetical heavy scalar particle, X, decaying into a singlet scalar particle, S, and a Standard Model Higgs boson, H, using 140 fb^{-1} of proton-proton collision data at the centre-of-mass energy of 13 TeV recorded with the ATLAS detector at the LHC is presented. The explored mass range is $300 \leq m_X \leq 1000$ GeV and $170 \leq m_S \leq 500$ GeV. The signature of this search is one or two leptons (e or μ) from the decay of vector bosons originating from the S particle, $S \to W^{\pm}W^{\mp}/ZZ$, and two photons from the Higgs boson decay, $H \to \gamma\gamma$. No significant excess is observed above the expected Standard Model background. The observed (expected) upper limits at the 95% confidence level on the cross-section for $gg \to X \to SH$, assuming the same $S \to WW/ZZ$ branching ratios as for a SM-like heavy Higgs boson, are between 530 (800) fb and 120 (170) fb.

Keywords: Hadron-Hadron Scattering , Higgs Physics

ArXiv ePrint: 2405.20926

https://doi.org/10.1007/JHEP10(2024)104

Contents

JHEP10(2024)104

1 Introduction

The Higgs boson was discovered by the ATLAS [1] and CMS [2] Collaborations in 2012 [3, 4]. Since then, an important goal has been to determine the Higgs boson properties and to perform precision measurements using proton-proton (pp) collision data from the Large Hadron Collider (LHC). Up until now, all measured properties are consistent with the Standard Model (SM) Higgs boson predictions [5, 6]. This discovery not only demonstrates the existence of the Higgs boson, but it also opens up new frontiers in particle physics that aim to address the limitations of the SM. There are a variety of beyond-the-SM scenarios that introduce additional scalar bosons such as the Next-to-Minimal Supersymmetric Standard Model (NMSSM) [7, 8], the Two-Real-Singlet Model (TRSM) [9, 10] or two-Higgs-Doublet Models (2HDM) [11].

The 2HDM+S model [12] extends the 2HDM hypothesis by considering the production of a heavy CP-even scalar boson (X) that could decay into an SM Higgs boson (H) and a hypothetical scalar singlet (S). A representative diagram of the $X \to SH$ production via gluon-gluon fusion is shown in figure 1. The $X \to SH$ branching ratio is assumed to be 100%.

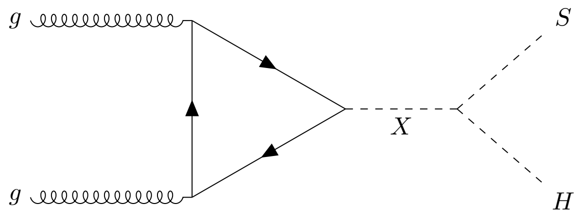

Figure 1. Illustrative Feynman diagram for $X \to SH$ production via gluon-gluon fusion.

Searches inspired by the 2HDM+S probing $X \to SS \to WW^*WW^*$ [13], $X \to SH \to bb\gamma\gamma$ [14] and $X \to SH \to VV\tau\tau$ [15], where V can be either a $W^\pm$ or Z boson, have been performed by the ATLAS Collaboration. For the latter, no significant excess is observed above the expected SM processes, and 95% confidence level (CL) upper limits are set on the signal production cross-section between 542 fb and 72 fb in the mass ranges $500 \leq m_X \leq 1500$ GeV and $200 \leq m_S \leq 500$ GeV [15]. The $X \to SH$ search in the $bb\gamma\gamma$ final state [14] set upper limits on the cross-section times the branching ratio ranging from 39 fb to 0.09 fb, over the mass ranges $170 \leq m_X \leq 1000$ GeV and $15 \leq m_S \leq 500$ GeV. The CMS Collaboration has also performed searches for $X \to SH$ in the $bb\gamma\gamma$ [16], $bb\tau\tau$ [17], and $4b$ [18] decay modes. In the diphoton plus two b-quarks search, the upper limits on the product of the production cross-section and the decay branching ratios of the signal process lie in the range of 0.9−0.04 fb [16], in the explored mass ranges $300 \leq m_X \leq 1000$ GeV and $90 \leq m_S \leq 800$ GeV. For the search with a pair of tau leptons and b-quarks in the final state, limits are set on the production cross-section ranging from 125 fb to 2.7 fb in the mass ranges $240 \leq m_X \leq 3000$ GeV and $60 \leq m_S \leq 2800$ GeV [17]. Comparable limits are found in the search involving four b-quarks in the final state, ranging from 150 to 0.1 fb in the mass ranges $0.9 \leq m_X \leq 4$ TeV and $60 \leq m_S \leq 600$ GeV [18]. All these results are obtained assuming for the S boson the same mass-dependent branching ratios as for the SM Higgs boson [19] (denoted SM-like branching ratios in the following).

This paper is focused on the search for $X \to SH \to VV\gamma\gamma$. The final state of interest is characterised by two photons from the SM Higgs boson decay ($H \to \gamma\gamma$), and one or two leptons (electrons or muons) originating from the vector bosons produced in the $S \to VV$ decays. This signature benefits from a good diphoton mass ($m_{\gamma\gamma}$) resolution [20] and the $m_{\gamma\gamma}$ distribution is used as the final discriminant. The requirement of at least one lepton rejects some SM background processes and therefore increases the signal-to-background ratio. The events are classified by the number and flavour of the leptons (electrons and muons) in the final state and multivariate analysis techniques are used to enhance the sensitivity of the search. The algorithm is trained to distinguish between the dominant SM backgrounds (multi-jet processes and vector bosons produced in association with a pair of photons) and the $X \to SH \to VV\gamma\gamma$ signal. This search is performed over the mass ranges $300 \leq m_X \leq 1000$ GeV and $170 \leq m_S \leq 500$ GeV. It allows to explore lower mass ranges than other final states with b-quarks where the signal becomes boosted at low m_S values, and suffer from low energetic b-quarks falling below the reconstructed threshold in the low m_X region. In the interpretation of the search results, the S boson is assumed to have SM-like branching ratios. Two additional scenarios wherein the S boson decays with a 100% branching ratio into a pair of $W^\pm$ or Z bosons, $S \to W^+W^-/ZZ$, are also considered.

JHEP10(2024)104

This paper is organised as follows. A brief description of the ATLAS detector is given in section 2. Data and simulation samples are described in section 3. The object reconstruction and event selection are outlined in section 4. The background estimation and the systematic uncertainties are described in section 5 and section 6, respectively. Section 7 presents the results of this search, which are summarised in section 8.

2 ATLAS detector

The ATLAS detector [1] at the LHC covers nearly the entire solid angle around the collision point.[1] It consists of an inner tracking detector surrounded by a thin superconducting solenoid, electromagnetic and hadronic calorimeters, and a muon spectrometer incorporating three large superconducting air-core toroidal magnets.

The inner-detector system (ID) is immersed in a 2 T axial magnetic field and provides charged-particle tracking in the range $|\eta| < 2.5$. The high-granularity silicon pixel detector covers the vertex region and typically provides four measurements per track, the first hit generally being in the insertable B-layer (IBL) installed before Run 2 [21, 22]. It is followed by the SemiConductor Tracker (SCT), which usually provides eight measurements per track. These silicon detectors are complemented by the transition radiation tracker (TRT), which enables radially extended track reconstruction up to $|\eta| = 2.0$. The TRT also provides electron identification information based on the fraction of hits (typically 30 in total) above a higher energy-deposit threshold corresponding to transition radiation.

The calorimeter system covers the pseudorapidity range $|\eta| < 4.9$. Within the region $|\eta| < 3.2$, electromagnetic calorimetry is provided by barrel and endcap high-granularity lead/liquid-argon (LAr) calorimeters, with an additional thin LAr presampler covering $|\eta| < 1.8$ to correct for energy loss in material upstream of the calorimeters. Hadronic calorimetry is provided by the steel/scintillator-tile calorimeter, segmented into three barrel structures within $|\eta| < 1.7$, and two copper/LAr hadronic endcap calorimeters. The solid angle coverage is completed with forward copper/LAr and tungsten/LAr calorimeter modules optimised for electromagnetic and hadronic energy measurements respectively.

The muon spectrometer (MS) comprises separate trigger and high-precision tracking chambers measuring the deflection of muons in a magnetic field generated by the superconducting air-core toroidal magnets. The field integral of the toroids ranges between 2.0 and 6.0 T m across most of the detector. Three layers of precision chambers, each consisting of layers of monitored drift tubes, cover the region $|\eta| < 2.7$, complemented by cathode-strip chambers in the forward region, where the background is highest. The muon trigger system covers the range $|\eta| < 2.4$ with resistive-plate chambers in the barrel, and thin-gap chambers in the endcap regions.

[1]ATLAS uses a right-handed coordinate system with its origin at the nominal interaction point (IP) in the centre of the detector and the z-axis along the beam pipe. The x-axis points from the IP to the centre of the LHC ring, and the y-axis points upwards. Polar coordinates (r, ϕ) are used in the transverse plane, ϕ being the azimuthal angle around the z-axis. The pseudorapidity is defined in terms of the polar angle θ as $\eta = -\ln\tan(\theta/2)$ and is equal to the rapidity $y = \frac{1}{2}\ln\left(\frac{E+p_z c}{E-p_z c}\right)$ in the relativistic limit. Angular distance is measured in units of $\Delta R \equiv \sqrt{(\Delta y)^2 + (\Delta\phi)^2}$.

The luminosity is measured mainly by the LUCID-2 [23] detector that records Cherenkov light produced in the quartz windows of photomultipliers located close to the beampipe.

Events are selected by the first-level trigger system implemented in custom hardware, followed by selections made by algorithms implemented in software in the high-level trigger [24]. The first-level trigger accepts events from the 40 MHz bunch crossings at a rate below 100 kHz, which the high-level trigger further reduces in order to record complete events to disk at about 1 kHz.

A software suite [25] is used in data simulation, in the reconstruction and analysis of real and simulated data, in detector operations, and in the trigger and data acquisition systems of the experiment.

3 Data and simulation samples

3.1 Data samples

The data used were collected with the ATLAS detector during 2015–2018, from pp collisions at a centre-of-mass energy $\sqrt{s} = 13$ TeV, corresponding to an integrated luminosity of 140 fb^{-1} with an uncertainty of 0.83% [26] after data quality requirements [27]. Events were recorded using diphoton triggers that require two reconstructed photon candidates with minimum transverse energies of 35 GeV and 25 GeV [28]. During the 2015–2016 data taking period, a *Loose* identification requirement was applied for this diphoton trigger while it was replaced by the *Medium* selection criteria to keep a tolerable trigger rate in 2017–2018 due to the increased instantaneous luminosity.

3.2 Monte Carlo simulated samples

3.2.1 Signal samples

The Monte Carlo (MC) simulated signal samples were produced with the Pythia 8 generator [29] with the matrix element calculation at leading order (LO) accuracy in quantum chromodynamics (QCD), followed by parton showering, hadronisation and underlying event modelling using the A14 set of tuned parameters ("tune") [30] and the NNPDF2.3lo parton distribution functions (PDF) [31]. During the sample generation, both X and S were assumed to have a narrow width compared with the experimental resolution, and their widths are fixed to 10 MeV. A total of 20 signal samples for various m_X and m_S were generated. The X boson was required to decay into S and H with S only decaying into a pair of W or Z bosons and H decaying into a pair of photons. By considering leptonic decays of W or Z bosons, the following three final state samples were produced for each m_X and m_S combination: $WW(\ell\nu q\bar{q}') + \gamma\gamma$, $WW(\ell\nu\ell\nu) + \gamma\gamma$, and $ZZ(\ell\ell q\bar{q}'/\ell\ell\nu\nu) + \gamma\gamma$ where $\ell = e$, μ, or τ. The $ZZ(4\ell) + \gamma\gamma$ decay sample is excluded due to its negligible contribution. To achieve a better signal generation efficiency, the samples were produced by requiring to have at least one lepton with transverse momentum (p_{T}) greater than 7 GeV and pseudorapidity $|\eta| < 3$ at the generator level.

JHEP10(2024)104

3.2.2 Background samples

The main background contributions result from SM single and double-Higgs boson production, forming a resonance on the diphoton mass ($m_{\gamma\gamma}$) spectrum, and other SM processes giving a smoothly falling $m_{\gamma\gamma}$ spectrum (continuum background). The corresponding events were generated with MC simulation.

Simulated events for single Higgs boson production via gluon-gluon fusion (ggF) were produced with the PowhegBox v2 generator [32–36] at next-to-next-to-leading order (NNLO) accuracy in QCD and interfaced with Pythia 8. The NNLO accuracy for arbitrary inclusive $gg \to H$ observables was achieved by reweighting the Higgs boson rapidity spectrum in Hj-MiNLO [37–39] to that of HNNLO [40]. The PDF4LHC15nnlo PDF set [41] and the AZNLO tune [42] of Pythia 8 were used and the decays of b- and c-hadrons were modelled by the EvtGen 1.6.0 programme [43]. These events were normalised using the NNLO cross-section in QCD plus electroweak corrections at next-to-leading order (NLO) [19, 44–53].

Simulated single Higgs boson events produced via vector-boson fusion (VBF) were generated with PowhegBox v2 at NLO accuracy in QCD and interfaced with Pythia 8. The PDF4LHC15nlo PDF set and AZNLO tune were used. Simulated events were normalised using an approximate-NNLO QCD cross-section with NLO electroweak corrections [54–56].

Events of single Higgs boson produced in association with a vector boson (VH, $V = W/Z$) were simulated using PowhegBox v2 and interfaced with Pythia 8. The Powheg prediction is accurate to NLO in QCD for VH+1jet distributions by using the MiNLO [57] prescription. The loop-induced $gg \to ZH$ process was generated separately at LO. The PDF4LHC15nlo PDF set and the AZNLO tune were used. Cross-sections calculated at NNLO in QCD with NLO electroweak corrections for $q\bar{q}/qg \to VH$ and at NLO and next-to-leading-logarithm accuracy in QCD for $gg \to ZH$ [58–64] were used for the normalisation of the MC samples.

Events corresponding to Higgs boson production in association with a pair of top or bottom quarks ($t\bar{t}H$ or $b\bar{b}H$) were simulated using PowhegBox v2 at NLO with the NNPDF3.0nlo PDF set [65]. The events were interfaced with Pythia 8 using the A14 tune and the NNPDF2.3lo PDF set. The decays of bottom and charm hadrons were performed with EvtGen 1.6.0.

Finally, events for single Higgs boson production in association with a single top quark were simulated with the MadGraph_aMC@NLO 2.3.3 [66] generator at NLO with the NNPDF3.0nlo PDF set. The events were interfaced with Pythia 8 using the A14 tune and the NNPDF2.3lo PDF set.

In addition to the single Higgs boson processes, events corresponding to the SM double Higgs boson ggF and VBF production modes are also considered. Those events were generated with PowhegBox v2 at NLO accuracy in QCD using the PDF4LHC15nlo PDF set and interfaced with Pythia 8. During the sample generation, one of the Higgs bosons was required to decay into two photons and the other Higgs boson was required to decay into WW, ZZ or $\tau\tau$, giving a final state with a pair of electrons or muons, or with one electron and one muon. Leptons were required to have $p_{\mathrm{T}} > 7\,\mathrm{GeV}$ and $|\eta| < 3$ at the generator level.

The normalisation of all Higgs boson samples accounts for the decay branching ratios calculated with HDECAY [67–69] and Prophecy4f [70–72].

Continuum background from $\gamma\gamma$+jets, $V+\gamma\gamma$, and $t\bar{t}+\gamma\gamma$ processes is considered. Their contributions are described with corresponding MC simulated samples that are exclusively used for the event selection optimisation. These samples were normalised with cross-sections as predicted by their corresponding MC generators.

Events from $\gamma\gamma$+jets production were simulated using the SHERPA 2.2.4 generator [73] at NLO accuracy in QCD with up to one additional parton and at LO with up to three additional partons. The matrix elements of these events were calculated with the Comix [74] and OPENLOOPS [75, 76] libraries and then matched to the SHERPA parton shower [77] using the MEPS@NLO prescription [78–81]. The NNPDF3.0NNLO PDF set [65] was used to describe the parton distributions in the incoming protons. A generator-level selection was applied to these events with the requirement of the invariant mass of the two photons to be between 90 GeV and 175 GeV.

The $V+\gamma\gamma$ events were generated using SHERPA 2.2.4 at NLO accuracy in QCD with up to one additional parton and up to three extra partons at LO. The calculation procedure is the same as in $\gamma\gamma$+jets event generation. Events were generated separately according to their final states as listed: $ee+\gamma\gamma$, $\mu\mu+\gamma\gamma$, $\tau\tau+\gamma\gamma$, $e\nu+\gamma\gamma$, $\mu\nu+\gamma\gamma$, $\tau\nu+\gamma\gamma$, and $\nu\nu+\gamma\gamma$. The generator-level photon p_{T} was required to be greater than 17 GeV and the invariant mass of the two photons should be larger than 80 GeV for these events.

The $t\bar{t}+\gamma\gamma$ process is simulated with the MADGRAPH5_AMC@NLO generator at LO and interfaced with PYTHIA 8. The NNPDF2.3LO PDF set and A14 tune were used for this production. The decays of bottom and charm hadrons were performed with EVTGEN 1.6.0.

In addition, dedicated samples (denoted "lepton-dependence samples") corresponding to final states of $\gamma\gamma+0\ell+\text{jets}$, $\gamma\gamma+1\ell+\text{jets}$, and $\gamma\gamma+2\ell+\text{jets}$ are generated to study the $m_{\gamma\gamma}$ distribution difference for cases with different lepton multiplicity at the generator level. These samples were produced with MADGRAPH5_AMC@NLO interfaced with PYTHIA 8. All possible SM processes with described final states except for those with $H\to\gamma\gamma$ were included in the event generation.

All simulated events except for the signals, $\gamma\gamma$+jets and lepton-dependence samples were passed through a detailed detector simulation of the ATLAS detector implemented with GEANT4 [82, 83]. The remaining samples were simulated using ATLFASTII [83], which exploys GEANT4 except for a parameterisation of the calorimeter response [84]. The effect of multiple interactions in the same and neighbouring bunch crossings (pile-up) was modelled by overlaying the simulated hard-scattering event with inelastic pp events generated with PYTHIA 8 [85] using the NNPDF2.3LO PDF set and the A3 tune [86]. A summary of MC simulated samples can be found in table 1.

4 Object and event selection

4.1 Object selection

Vertices from pp collisions are reconstructed if they have associated at least two ID tracks with $p_{\mathrm{T}} > 0.5$ GeV. The diphoton primary vertex (PV) is chosen by using a neural network algorithm that uses information about the ID tracks as well as the photon candidates [87].

JHEP10(2024)104

Process	Generator	PDF	Tune
	Signal		
$X \to SH \to VV + \gamma\gamma$	PYTHIA 8	NNPDF2.3LO	A14
	SM Single and double Higgs boson production		
ggF H	POWHEG+PYTHIA 8	PDF4LHC15NNLO	AZNLO
VBF H	POWHEG+PYTHIA 8	PDF4LHC15NLO	AZNLO
WH	POWHEG+PYTHIA 8	PDF4LHC15NLO	AZNLO
$qq \to ZH$	POWHEG+PYTHIA 8	PDF4LHC15NLO	AZNLO
$gg \to ZH$	POWHEG+PYTHIA 8	PDF4LHC15NLO	AZNLO
$t\bar{t}H$	POWHEG+PYTHIA 8	NNPDF3.0NLO	A14
$b\bar{b}H$	POWHEG+PYTHIA 8	NNPDF3.0NLO	A14
$tHbj$	MADGRAPH_AMC@NLO+PYTHIA 8	NNPDF3.0NLO	A14
tHW	MADGRAPH_AMC@NLO+PYTHIA 8	NNPDF3.0NLO	A14
ggF $HH \to VV + \gamma\gamma$	POWHEG+PYTHIA 8	PDF4LHC15NLO	A14
VBF $HH \to VV + \gamma\gamma$	POWHEG+PYTHIA 8	PDF4LHC15NLO	A14
	Continuum background		
$\gamma\gamma +$ jets	SHERPA	NNPDF3.0NNLO	—
$V + \gamma\gamma$	SHERPA	NNPDF3.0NNLO	—
$t\bar{t}\gamma\gamma$	MADGRAPH_AMC@NLO+PYTHIA 8	NNPDF3.0NLO	A14
	Lepton-dependence samples		
$\gamma\gamma + 0\ell +$ jets	MADGRAPH_AMC@NLO+PYTHIA 8	NNPDF3.0NLO	A14
$\gamma\gamma + 1\ell +$ jets	MADGRAPH_AMC@NLO+PYTHIA 8	NNPDF3.0NLO	A14
$\gamma\gamma + 2\ell +$ jets	MADGRAPH_AMC@NLO+PYTHIA 8	NNPDF3.0NLO	A14

Table 1. Summary of MC simulated samples used in this analysis.

Photons are reconstructed based on a dynamic, topological cell clustering-based algorithm from the energy deposits in the electromagnetic calorimeter in the region $|\eta| < 2.37$, excluding the transition region between the barrel and endcap calorimeters $1.37 < |\eta| < 1.52$ [88]. The photon identification criteria is constructed using information from the shower shapes and the primary identification criteria is labelled as *Tight*. The photon isolation criteria quantifies the activity near the photons from the tracks of nearby charged particles, or from energy deposits in the calorimeter [88]. This analysis considers events by selecting photon candidates which are required to satisfy a set of preselection criteria. The two photons with the highest transverse momentum, referred to as leading (γ_1) and subleading (γ_2) photons, must satisfy $p_T > 22$ GeV and $|\eta| < 2.37$, excluding the transition region between the barrel and endcap calorimeters $1.37 < |\eta| < 1.52$. Photon candidates are separated from multi-jet backgrounds by applying *Tight* identification and further isolation requirements to suppress jets misidentified as photons.

Electrons are reconstructed and identified based on clusters built from energy deposits in the electromagnetic calorimeter, which are matched to a track in the inner detector [88]. The muon reconstruction is performed using information from the inner detector and muon spectrometer, as well as the electromagnetic and hadronic calorimeters [89]. In this search, electron candidates are required to have $p_T > 10$ GeV and $|\eta| < 2.47$, excluding the transition region between the barrel and endcap calorimeters $1.37 < |\eta| < 1.52$. Muon candidates should have $p_{\mathrm{T}} > 10\,\mathrm{GeV}$ and $|\eta| < 2.7$. Leptons must satisfy *Medium* identification and *Loose* isolation [88, 89], and a set of requirements based on the longitudinal and transverse impact parameters relative to the vertex and the beam axis.

Jets are reconstructed using a particle flow algorithm [90] from noise-suppressed positive-energy topological clusters [91] in the calorimeter using the anti-k_t algorithm [92, 93] with a radius parameter $R = 0.4$. The jet energy scale calibration restores the jet p_{T}, energy, and mass to that of jets reconstructed at particle level [94]. In this search, jets are required to have $p_{\mathrm{T}} > 25\,\mathrm{GeV}$ and to be in the central region of the detector, $|\eta| < 2.5$. To suppress jets from pileup, a jet-vertex-tagger multivariate discriminant [95] is applied to jets with $p_{\mathrm{T}} < 60\,\mathrm{GeV}$. Jets containing b-hadrons are identified (b-tagged) using the 77% efficiency working point of the DL1r b-tagging algorithm [96].

An overlap removal procedure is performed to avoid double-counting objects. First, electrons overlapping with any of the two selected photons ($\Delta R < 0.4$) are removed. Jets overlapping with the selected photons ($\Delta R < 0.4$) or electrons ($\Delta R < 0.2$) are removed. Electrons overlapping with the remaining jets ($\Delta R < 0.4$) are removed to match the requirements imposed when measuring isolated electron efficiencies. Finally, muons overlapping with photons or jets ($\Delta R < 0.4$) are removed.

The missing transverse momentum, with magnitude $E_{\mathrm{T}}^{\mathrm{miss}}$, is defined as the negative vector sum of the transverse momenta of the selected photon, electron, muon, and jet objects, as well as of the transverse momenta of remaining low-p_{T} particles estimated by using tracks associated with the diphoton primary vertex but not assigned to any of the selected objects [97].

The above requirements constitute the event preselection of this search.

4.2 Event selection

This search selects events with two photons from the Higgs boson decay, and one or two leptons coming from the vector bosons originated from the $S \to VV$ process. Events are required to pass diphoton triggers as described in section 3. Moreover, photons are required to have $p_{\mathrm{T}}^{\gamma_{1(2)}}/m_{\gamma\gamma} > 0.35$ (0.25) [20]. Selected events must contain one or two additional leptons (e or μ) with $p_{\mathrm{T}} > 10\,\mathrm{GeV}$. To suppress backgrounds with top quarks, events containing one or more b-tagged jets are rejected.

The events are classified into four different regions depending on the number and flavour of leptons originating from the vector boson decays in the $S \to W^{\pm}W^{\mp}$ and $S \to ZZ$ processes. Events in the one-lepton (1ℓ) region are required to have one lepton and at least two jets. The other regions account for events with two leptons with opposite electric charge. Events with two leptons of different flavour are targeted in the $e\mu$ region. Events having two leptons of same flavour (SF) are further split by checking the compatibility of the dilepton invariant mass with the Z-mass pole. Events with at least two jets and satisfying $|m_{\ell\ell} - 91.2\,\mathrm{GeV}| < 10\,\mathrm{GeV}$ are classified in the $2\ell(ZZ)$ region, which targets the $S \to ZZ \to \ell\ell$+jets process. The remaining SF events are included in the $2\ell(WW)$ region.

Two optimisation strategies are adopted. For each of the 1ℓ and $2\ell(WW)$ regions, a Boosted Decision Tree (BDT) is used to enhance the analysis sensitivity. The 1ℓ and $2\ell(WW)$ regions further split the events by dividing the BDT output distribution into the loose (low BDT score) and tight (high BDT score) signal regions. The $e\mu$ and $2\ell(ZZ)$ signal regions are

JHEP10(2024)104

Preselection	Two photon candidates and no b-tagged jets			
Region	1ℓ	$e\mu$	$2\ell(WW)$	$2\ell(ZZ)$
Number of leptons	1	2	2	2
Total electric charge	–	0	0	0
Same flavour leptons	–	No	Yes	Yes
$\lvert m_{\ell\ell} - m_Z \rvert$ [GeV]	–	–	> 10	< 10
Number of jets	≥ 2	–	–	≥ 2
Strategy	BDT	Cut-based	BDT	Cut-based
Number of signal regions	2	1	2	1
$m_{\gamma\gamma}$ region	$[105, 160]$ GeV			

Table 2. Event selection and classification strategy.

limited in statistics and have higher signal-over-background ratios than the BDT-based regions. Due to this, the $e\mu$ and $2\ell(ZZ)$ signal regions follow an inclusive cut-based strategy and events are not further split into sub-regions. This analysis strategy results in six signal regions.

The final discriminant of this search is the diphoton invariant mass spectrum. To be consistent with the $H \to \gamma\gamma$ process and to exclude the region of the Z-boson resonance, the range of $m_{\gamma\gamma}$ is limited to the $[105, 160]$ GeV region. The signal region is defined as the $m_{\gamma\gamma}$ within $[120,\ 130]$ GeV. Events outside the signal region, referred to as sideband events, are used to estimate the main background processes as described in section 5. After all selections described above are applied, the combined acceptance and selection efficiency for the signal production ranges from 11% to 25%, which increases for higher m_X hypotheses. Table 2 summarises the event selection and strategy for each of the signal regions.

4.3 Boosted Decision Tree strategy

The dominant signal process in this search is the $S \to W^+W^-$ decay given the larger branching ratio compared with the $S \to ZZ$ process for the explored m_S range. In the 1ℓ region one of the W bosons decays leptonically and the other decays hadronically. In the $e\mu$ and $2\ell(WW)$ regions both W bosons decay leptonically resulting into a pair of leptons with different and same flavour, respectively. Two BDTs are built based on the kinematic observables from the final-state objects in the 1ℓ and $2\ell(WW)$ regions. The different signal samples are grouped according to the S mass into four groups: $m_S = 170$ GeV, $m_S = 200$ GeV, $m_S = 300$ GeV and $m_S = 400, 500$ GeV. These groups contain from four to six signal samples depending on the m_X values in each group. The BDT algorithms are trained for each group against the total background from MC simulation using the parameterised BDT method [98].

Twelve and nine variables for the 1ℓ and $2\ell(WW)$ regions respectively are used to train each BDT, as listed in table 3. The BDT input variables list excludes $m_{\gamma\gamma}$ as it is used as the main discriminant; these variables are selected to have small correlation with $m_{\gamma\gamma}$. The BDT variable with the highest separation power is the transverse momentum of the pairs of photons from the SM Higgs boson decay ($p_{\mathrm{T}}^{\gamma\gamma}$). The comparison of the $p_{\mathrm{T}}^{\gamma\gamma}$ distributions for data, the expected SM background processes and the $(m_X,\, m_S) = (1000,\, 300)$ GeV signal from simulation is shown in figure 2 for the 1ℓ and $2\ell(WW)$ regions.

Variable	Description	BDT-based regions	
		1ℓ	$2\ell(WW)$
$\Delta R(\gamma\gamma, \ell\nu jj)$	ΔR between the diphoton system and the $\ell + E_{\mathrm{T}}^{\mathrm{miss}} jj$ system	10	
$\Delta R(\gamma\gamma, \ell\nu\ell\nu)$	ΔR between the diphoton system and the $\ell\ell + E_{\mathrm{T}}^{\mathrm{miss}}$ system		9
$\Delta R(jj, \ell\nu)$	ΔR between the dijet system and the $\ell + E_{\mathrm{T}}^{\mathrm{miss}}$ system	9	
$\Delta R(\ell_1\nu, \ell_2)$	ΔR between leading lepton + $E_{\mathrm{T}}^{\mathrm{miss}}$ and subleading lepton		8
$p_{\mathrm{T}}^{\ell+E_{\mathrm{T}}^{\mathrm{miss}}jj}$	p_{T} of the $\ell + E_{\mathrm{T}}^{\mathrm{miss}} jj$ system	2	
$p_{\mathrm{T}}^{\gamma\gamma}$	p_{T} of the diphoton system	1	2
$\Delta\phi(\gamma\gamma, \ell_{(1)})$	$\Delta\phi$ between the diphoton system and the (leading) lepton	12	7
$\Delta R(\ell, E_{\mathrm{T}}^{\mathrm{miss}})$	ΔR between the lepton and the $E_{\mathrm{T}}^{\mathrm{miss}}$	8	
$p_{\mathrm{T}}^{\ell_{(1)}}$	p_{T} of the (leading) lepton	4	4
$p_{\mathrm{T}}^{\ell_1+E_{\mathrm{T}}^{\mathrm{miss}}}$	p_{T} of the leading lepton and $E_{\mathrm{T}}^{\mathrm{miss}}$ system		3
$m_{\mathrm{T}}(\ell_{(1)} E_{\mathrm{T}}^{\mathrm{miss}})$	Transverse mass of the (leading) lepton and $E_{\mathrm{T}}^{\mathrm{miss}}$	11	5
$m_{\ell\ell}$	Invariant mass of the dilepton system		6
$E_{\mathrm{T}}^{\mathrm{miss}}$	Missing transverse energy	3	1
$\Delta R(j, j)$	ΔR between the two jets with closest mass to m_W	6	
p_{T}^{jj}	p_{T} of the the two jets with closest mass to m_W	5	
m_{jj}	Invariant mass of the dijet system with closest mass to m_W	7	

Table 3. Variables used as inputs to the BDT in the 1ℓ and $2\ell(WW)$ regions. The highest-p_{T} (leading) lepton is denoted ℓ_1, and the subleading lepton is denoted ℓ_2. The numbers indicate the ranking of each input variable, with 1 corresponding to the most highly ranked variable.

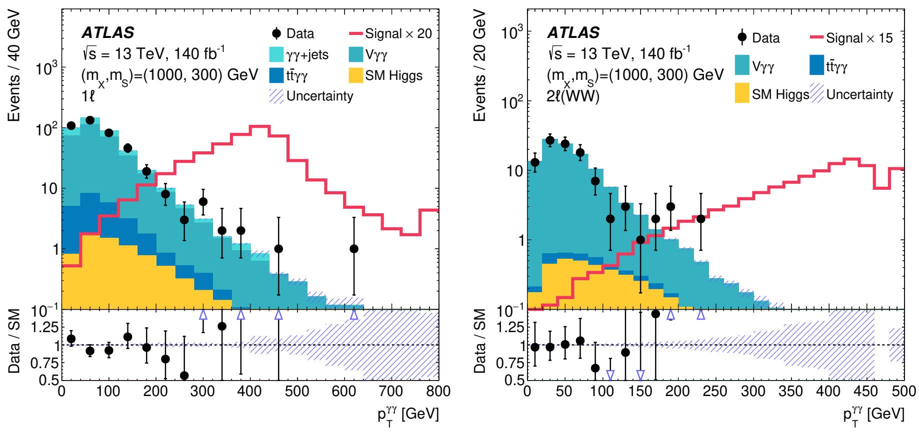

(a) (b)

Figure 2. Transverse momentum of the diphoton system, $p_{\mathrm{T}}^{\gamma\gamma}$, in the (a) 1ℓ and (b) $2\ell(WW)$ regions for data and the expected SM background from simulation after the event selection is applied. The $V\gamma\gamma$ and $\gamma\gamma$+jets simulated background is scaled to match the data yield excluding the $120 < m_{\gamma\gamma} < 130$ GeV region. The contribution from the SM single and double Higgs boson processes (denoted "SM Higgs"), which is estimated from the MC simulation, is also shown. The $(m_X, m_S) = (1000, 300)$ GeV signal prediction (open red histogram) for the scenario of SM-like $\mathscr{B}(S \to WW/ZZ)$ is also shown, normalised to a cross-section corresponding to the 95% CL upper limit shown in figure 6. An additional normalisation factor, as indicated in the legend, is applied to scale the signal for visibility. The last bin in each distribution contains the overflow.

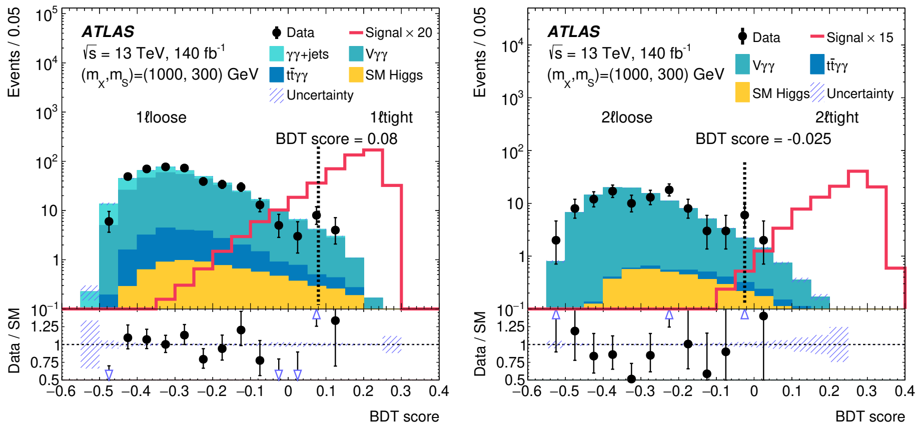

(a) (b)

Figure 3. BDT output distributions in the (a) 1ℓ and (b) $2\ell(WW)$ regions for data and the expected SM background from simulation after the event selection is applied. The $V\gamma\gamma$ and $\gamma\gamma$+jets simulated background is scaled to match the data yield excluding the $120 < m_{\gamma\gamma} < 130$ GeV region. The contribution from the SM single and double Higgs boson processes (denoted "SM Higgs"), which is estimated from the MC simulation, is also shown. The $(m_X, m_S) = (1000, 300)$ GeV signal prediction (open red histogram) for the scenario of SM-like $\mathscr{B}(S \to WW/ZZ)$ is also shown, normalised to a cross-section corresponding to the 95% CL upper limit shown in figure 6. An additional normalisation factor, as indicated in the legend, is applied to scale the signal for visibility. The BDT score threshold values are represented by the dashed vertical lines. The shaded band represents the statistical uncertainty on the background prediction. The last bin in each distribution contains the overflow.

Figure 3 shows the BDT output distributions for data, the expected SM background processes and the $(m_X, m_S) = (1000, 300)$ GeV signal from simulation. The BDT output discriminant is used to further split events in loose and tight BDT regions: 1ℓloose and 1ℓtight regions are defined for the 1ℓ region, as well as 2ℓloose and 2ℓtight signal regions for the $2\ell(WW)$ region. The BDT score threshold values used range from -0.1 to 0.2 depending on the signal mass hypothesis, and result from a scan using the root square of the signal significance in each region added in quadrature: $Z_{\text{comb}} = \sqrt{Z^2_{\text{loose}} + Z^2_{\text{tight}}}$, being

$$Z_{\text{loose/tight}} = \sqrt{2 \times \left[(s+b) \times \left(\ln \frac{s+b}{b}\right) - s\right]_{\text{loose/tight}}}, \tag{4.1}$$

where s represents the signal event yields and b is the background yield in each BDT region. Both signal and background yields are calculated by considering events in the region of $120 < m_{\gamma\gamma} < 130$ GeV. The selected threshold values are established by maximising Z_{comb} under the requirement of the presence of at least one sideband data event in the tight BDT regions. Table 4 shows the SM expected event yields, estimated as detailed in section 5, and the observed data for each of the analysis regions. The expected signal yields for $(m_X, m_S) = (1000, 300)$ GeV, considering a $gg \to X \to SH$ production cross-section of 1 pb, are provided for comparison. The S scalar boson is assumed to decay into other SM particles with the same mass-dependent branching ratios of the SM Higgs boson.

JHEP10(2024)104

	BDT-based regions				Cut-based regions	
	1ℓtight	1ℓloose	2ℓtight	2ℓloose	$2\ell(ZZ)$	$e\mu$
Continuum	6.0 $\pm$ 2.4	405 $\pm$ 20	2.0 $\pm$ 1.4	100 $\pm$ 10	2.0 $\pm$ 1.4	2.0 $\pm$ 1.4
SM Higgs	0.55 $\pm$ 0.08	6.8 $\pm$ 0.9	0.46 $\pm$ 0.06	3.35 $\pm$ 0.46	0.52 $\pm$ 0.08	0.24 $\pm$ 0.03
Total background	6.6 $\pm$ 2.8	412 $\pm$ 23	2.46 $\pm$ 1.6	103 $\pm$ 11	2.52 $\pm$ 1.6	2.24 $\pm$ 1.5
Signal (m_X, m_S) (1000, 300) GeV	20.9 $\pm$ 2.4	2.90 $\pm$ 0.34	2.96 $\pm$ 0.35	0.016 $\pm$ 0.002	2.03 $\pm$ 0.24	2.08 $\pm$ 0.24
Data	6	405	2	100	2	2

Table 4. Observed data and expected event yields for the different analysis regions after the full selection from table 2 is applied. The continuum background includes the $V\gamma\gamma$, $\gamma\gamma$+jets and $t\bar{t}\gamma\gamma$ processes estimated as described in section 5. The contribution from the SM single and double Higgs boson processes (denoted "SM Higgs") is estimated from simulation. The uncertainties include all sources of systematic uncertainty described in section 6. Event yields for the $(m_X, m_S) = (1000, 300)$ GeV signal are also shown assuming $\sigma(gg \to X \to SH) = 1$ pb and SM-like $\mathscr{B}(S \to WW/ZZ)$.

5 Background estimation

Background processes can be classified into "resonant" or "continuum" based on their $m_{\gamma\gamma}$ spectrum. The SM Higgs boson single and pair production events form the resonant background component. These processes are purely estimated from MC simulation.

The continuum background component arises mostly from multi-jet processes associated with two photons ($\gamma\gamma$+jets), and vector boson or top-antitop-quark production in association with a pair of photons ($V + \gamma\gamma$ and $t\bar{t}\gamma\gamma$). Contributions from these processes are checked with the MC simulated samples as described in section 3.2.2 and used for the event selection optimisation. No dedicated MC simulated events are produced for processes with small contribution such as VV+$\gamma\gamma$ or processes with jets or leptons misidentified as photons. Their contributions are included in the data-driven background, which accounts for all possible processes. The contribution from the continuum background is estimated from a fit to the data $m_{\gamma\gamma}$ distribution in the sideband region with a template. This template is generated from an analytic function that is obtained from a fit to the $m_{\gamma\gamma}$ distribution in a dedicated data control region due to low statistics of sideband data in the signal region. These control regions are defined by requiring zero leptons and at least two photons passing looser identification and isolation criteria but failing the signal region photon selections as described in section 4.1. Two different control samples are defined based on the number of leptons in each signal region using the selected jet to mimic the lepton behaviour. The control sample for the $\gamma\gamma + 1\ell$ region selects events with a pair of photons accompanied by one jet. For the other signal regions with a pair of leptons in the final state, the control sample requires the presence of at least two jets. A schematic diagram presenting the definitions of different regions is shown in figure 4. The fitted $m_{\gamma\gamma}$ shape difference between the signal region and control region is considered as a systematic uncertainty in the background shape estimation. In addition, the $m_{\gamma\gamma}$ shape difference related to the number of leptons in the generator-level is also evaluated and included as a systematic uncertainty. This uncertainty is estimated by comparing the fit results to the full $m_{\gamma\gamma}$ mass range distributions in the control region and the validation region using dedicated lepton-dependence MC samples as described in section 3.2.2, where

JHEP10(2024)104

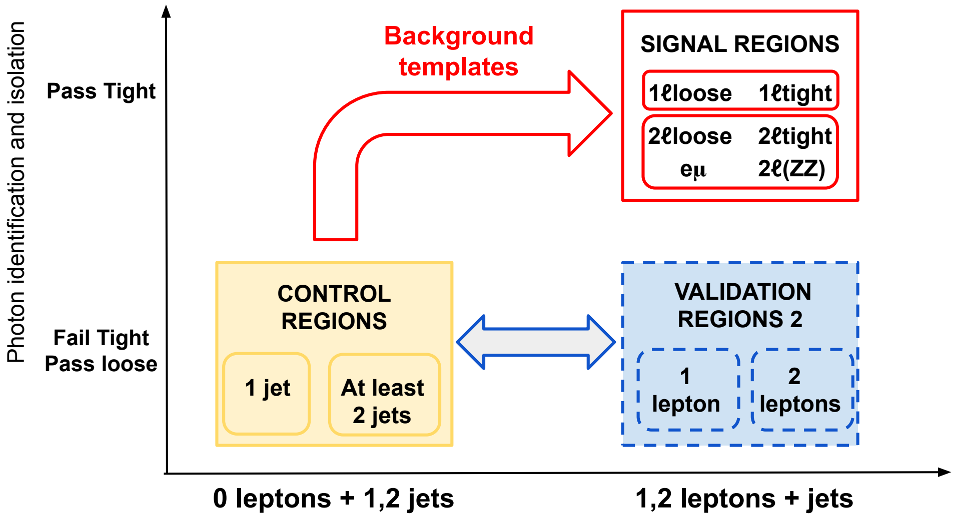

Figure 4. Definition of signal and control regions. The red arrow represents the $m_{\gamma\gamma}$ template generated in the 0-lepton control region which is applied to the signal regions. The systematic uncertainty in the background shape, obtained from differences between the control and the validation regions, is indicated by the blue arrow.

the validation region is defined by applying almost the same event selections as the signal region but inverting identification and isolation requirements as same as in the control region.

Three types of analytic functions are explored: exponential function, exponential function of a 2$^{\text{nd}}$ order polynomial, and a Chebyshev polynomial of order $n = 1, \ldots, 5$. The functional form is chosen via a spurious signal test as described in ref. [99]. The spurious signal is extracted by performing a signal-plus-background fit to the data $m_{\gamma\gamma}$ distribution in the control region (denoted "background-only" template), which is assumed to only include contributions from continuum background processes. The selection criteria follow the strategy as documented in ref. [20]. The spurious signal should be less than 20% of the background uncertainty. In addition to the spurious signal requirement, the goodness of the fit with background functional form to the background-only template is evaluated with a χ^2 test and the corresponding p-value is required to be greater than 5%. When multiple functions pass the criteria, the one with the smallest degrees of freedom is chosen. The corresponding spurious signal for the selected function is treated as the systematic uncertainty due to background modelling with the analytic function. In total 80 continuum background functions are estimated corresponding to various signal regions. Of these 80 functions, 78 are exponential functions of 2$^{\text{nd}}$ order polynomials and the remaining two are simple exponential functions. Due to the low statistics in the $e\mu$ and $2\ell(ZZ)$ signal regions and the fact that the $m_{\gamma\gamma}$ distribution shows a negligible dependence on the flavour of leptons, the continuum background shape estimated in the 2ℓtight region is also applied to these two regions.

6 Systematic uncertainties

Systematic uncertainties arise from the theory modelling of signal and background, the detector simulation and instrumental effects, and the estimation of the continuum background.

6.1 Theoretical uncertainties

Theoretical uncertainties are considered for signal and the SM single and double Higgs boson backgrounds. Uncertainties from six sources are considered: from PDF set and strong coupling constant α_S, from the QCD factorisation and renormalisation scales (μ_F and μ_R), and from the parton shower parameters and hadronisation models.

To evaluate the impact of varying the PDF set choice and α_S value, event weights corresponding to alternative PDF sets and α_S values are generated for each event along with the nominal weight. Effects on signal region yields are considered as systematic uncertainties. Variations on signal and SM Higgs boson yields are found to be 6% and 4% respectively.

The systematic uncertainty due to higher-order QCD effects is estimated by independently varying the QCD factorisation and renormalisation scales up and down from their nominal values by a factor of two, taking the envelope of the 7-point variation. Their impacts on signal and SM Higgs boson background yields are about 9% and 13% respectively.

The uncertainty due to the parton shower and hadronisation model is estimated by comparing the yields from the nominal MC samples using PYTHIA 8, with alternative samples using instead HERWIG 7. The corresponding uncertainties in the signal and Higgs boson background yields are 5% and 3% respectively.

6.2 Experimental uncertainties

Systematic uncertainties arising from the luminosity determination, pileup modelling, and trigger, reconstruction and selection efficiencies, as well as energy scales and resolutions, are considered for signal, single and double Higgs boson events. Their impacts on both the normalisation and shape are included in the statistical analysis for the final results.

The uncertainty in the integrated luminosity for 2015–2018 data taking period is 0.83% [26], obtained using the LUCID-2 detector for the primary luminosity measurement, complemented by measurements using the inner detector and calorimeters.

The uncertainty in the modelling of the pileup distribution in the simulation is estimated to have 2%–3% impacts on yields of signal, single and double Higgs boson events.

The photon reconstruction, identification and isolation efficiencies are measured using three data-driven techniques as mentioned in ref. [100]. Their effects on yields and shapes are estimated by varying the measured efficiency scale factors between data and simulation, resulting in less than 2% variations for signal yields. Uncertainties in the photon energy scale and resolution described in ref. [88] are considered as well. These uncertainties affect the signal yield less than 0.5%; a similar impact is found for single Higgs boson and double Higgs bosons events. The uncertainty in the photon trigger efficiency is also considered and its impact on event yields is found to be negligible.

Uncertainties in the electron reconstruction, identification and isolation efficiencies are reported in ref. [100]. They affect the signal and SM Higgs boson yields by about 2%. Uncertainties in electron energy scale and resolution are also evaluated and found to have a negligible impact.

In addition, uncertainties in muon reconstruction, identification, isolation efficiencies as well as the muon momentum scale and resolution [89], and uncertainties in the jet energy scale and resolution [94] are also considered. Furthermore, uncertainties arising from jet

JHEP10(2024)104

property selections: jet-vertex-tagger [95] and b-jet tagging [101–103] are included. Finally, the uncertainty related to $E_{\mathrm{T}}^{\mathrm{miss}}$ resulting from tracks not associated with the selected objects [97] is considered. All these uncertainties were found to have a negligible impact on the signal and SM Higgs boson yields.

6.3 Continuum background modelling uncertainty

The continuum background estimation (see section 5) assumes no significant shape differences between the control region (events with no leptons) and the signal region (events with at least one lepton). An uncertainty (called lepton-dependence uncertainty) associated with the background modelling is evaluated by comparing the shape of the $m_{\gamma\gamma}$ distribution in $\gamma\gamma + 0\ell$ events with that in $\gamma\gamma + \ell\nu$jj and $\gamma\gamma + \ell\nu\ell\nu$ events from dedicated MC simulated samples (see section 3.2.2). The variations between diphoton events with and without leptons are computed using the $m_{\gamma\gamma}$ distribution in the $[105, 160]$ GeV range. The average variation over all bins is about 2% for all signal regions. In addition to lepton-dependence uncertainty, a 2% uncertainty arises from the comparison of the shape of the $m_{\gamma\gamma}$ distribution in the control and the signal regions. The systematic uncertainty arising from a potential bias from the background shape functional form choice is accounted by the spurious signal uncertainty (see section 5).

7 Results

The contribution of a potential signal in the data is extracted through a simultaneous fit to the $m_{\gamma\gamma}$ distributions in all six signal regions, which is implemented with the RooFit [104] and RooStats [105] frameworks. The fit is performed with a binned likelihood model built from the product of the Poission distribution in each bin and region, and including Gaussian distributions to describe the effect of systematic uncertainties. For each $m_{\gamma\gamma}$ distribution, 22 equal width bins in a range of 105 GeV to 160 GeV are used in the fit. The parameter-of-interest is $\sigma(gg \to X) \times \mathscr{B}(X \to SH)$ and is left unconstrained in the fit. The shape of the signal for each individual region is obtained from simulated events. Contributions from the single and double Higgs boson processes are estimated from MC simulated samples with their normalisation fixed to SM predictions. Theoretical and experimental uncertainties corresponding to both the signal and the Higgs boson backgrounds are included in the fit and controlled by the nuisance parameters. For the continuum background, the shape is estimated with the method described in section 5 and kept fixed in the fit, while its normalisation is left unconstrained. In total four individual normalisation factors are included corresponding to 1ℓtight, 1ℓloose, 2ℓtight and 2ℓloose, respectively. The $e\mu$ and $2\ell(ZZ)$ regions share the same normalisation factor for continuum background as the 2ℓtight region. Background shape uncertainty and the spurious signal uncertainty are also considered in the fit and described by the corresponding nuisance parameters. To improve the robustness of the fit, any systematic uncertainty with less than 0.5% impact on either shape or yield is removed from the fit model. With such requirement, only uncertainties related to photon and electron, pileup reweighting, theory, and continuum background estimation are left, and others are ignored during the fit.

Three scenarios are considered for the final results corresponding to three hypotheses on the $S \to WW/ZZ$ branching ratios: SM-like $\mathscr{B}(S \to WW/ZZ)$ [19], $\mathscr{B}(S \to WW) = 100\%$, and $\mathscr{B}(S \to ZZ) = 100\%$.

JHEP10(2024)104

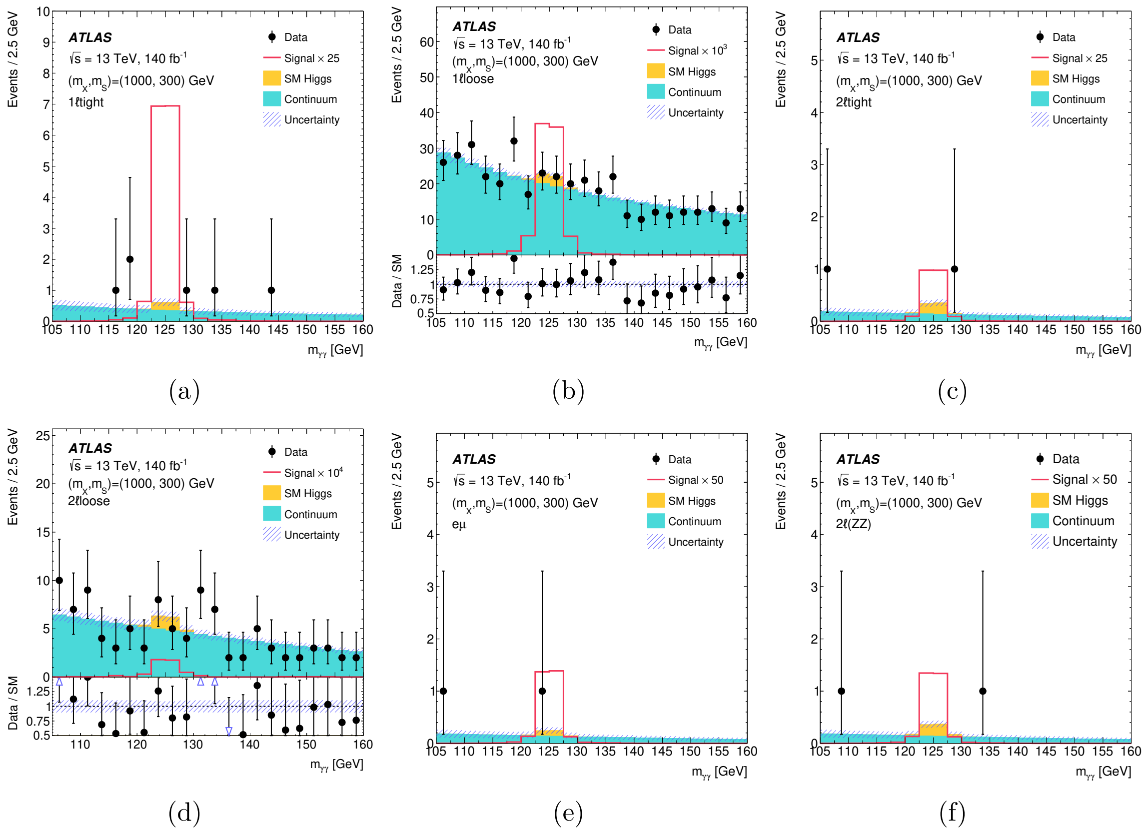

Figure 5. Distribution of $m_{\gamma\gamma}$ after the signal-plus-background fit to data in the (a) 1ℓtight, (b) 1ℓloose, (c) 2ℓtight, (d) 2ℓloose, (e) $e\mu$ and (f) $2\ell(ZZ)$ regions. The contribution from the SM single and double Higgs boson processes (denoted "SM Higgs"), which is estimated from the MC simulation, is shown added on top of the continuum background distribution. The $(m_X, m_S) = (1000, 300)$ GeV signal prediction (open red histogram) for the scenario of SM-like $\mathscr{B}(S \to WW/ZZ)$ is also shown, normalised to a cross-section corresponding to the 95% CL upper limit shown in figure 6. An additional normalisation factor, as indicated in the legend, is applied to scale the signal for visibility.

Figure 5 presents the $m_{\gamma\gamma}$ distributions in the six signal regions after performing the signal-plus-background fit corresponding to a signal with $m_X = 1000$ GeV and $m_S = 300$ GeV for the SM-like $\mathscr{B}(S \to WW/ZZ)$ scenario. Other branching-ratio scenarios and signal-mass hypotheses are also tested and no deviation with respect to the SM background expectation is observed. Consequently, 95% CL upper limits are set on $\sigma(gg \to X) \times \mathscr{B}(X \to SH)$ for each branching-ratio scenario and signal-mass hypothesis using the profile likelihood ratio technique with the asymptotic approximation [106] and the CL_s [107, 108] method. The results are validated using pseudo-experiments and found to agree within 20%.

Figure 6 shows the 95% CL observed and expected limits on $\sigma(gg \to X) \times \mathscr{B}(X \to SH)$ as a function of m_X and m_S for the SM-like $\mathscr{B}(S \to WW/ZZ)$ scenario. The observed (expected) limit ranges from 530 fb (800 fb) to 120 fb (170 fb) depending on the scalar masses. The results are dominated by the 1ℓtight region, with the other regions contributing with comparably lower sensitivity. In the 1ℓtight region, a slight deficit in the data yield compared to the background expectation is observed across all mass hypotheses, which leads to a better observed limit than the expected one for every mass point.

JHEP10(2024)104

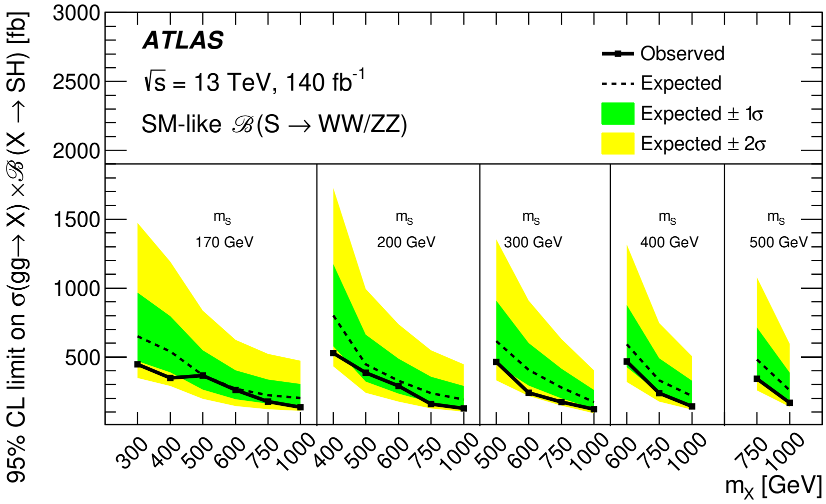

Figure 6. Observed (solid line) and expected (dashed line) 95% CL upper limits on $\sigma(gg \to X) \times \mathscr{B}(X \to SH)$ as a function of m_X and m_S, under the assumption of SM-like $\mathscr{B}(S \to WW/ZZ)$. The green and yellow shaded areas indicate the ± 1 and ± 2 standard deviations around the expected limit.

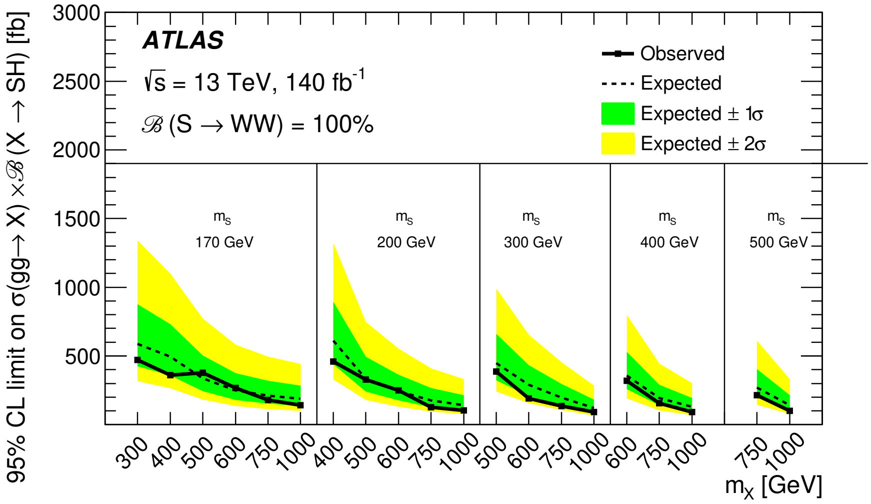

Figure 7. Observed (solid line) and expected (dashed line) 95% CL upper limits on $\sigma(gg \to X) \times \mathscr{B}(X \to SH)$ as a function of m_X and m_S, under the assumption of $\mathscr{B}(S \to WW) = 100\%$. The green and yellow shaded areas indicate the ± 1 and ± 2 standard deviations around the expected limit.

Limits corresponding to assumptions of the scalar S with a 100% decay branching ratio to WW or ZZ are derived and presented in figures 7 and 8. Under the assumption that $\mathscr{B}(S \to WW) = 100\%$, the observed limit varies from 470 fb to 91 fb whereas the expected limit ranges from 610 fb to 120 fb. The upper limits under the scenario $\mathscr{B}(S \to ZZ) = 100\%$ are significantly higher: from 1530 fb to 360 fb for observed limits and from 2160 fb to 510 fb for expected limits. The analysis sensitivity is limited by the statistical uncertainty, with systematic uncertainties degrading the expected limits by about 2%.

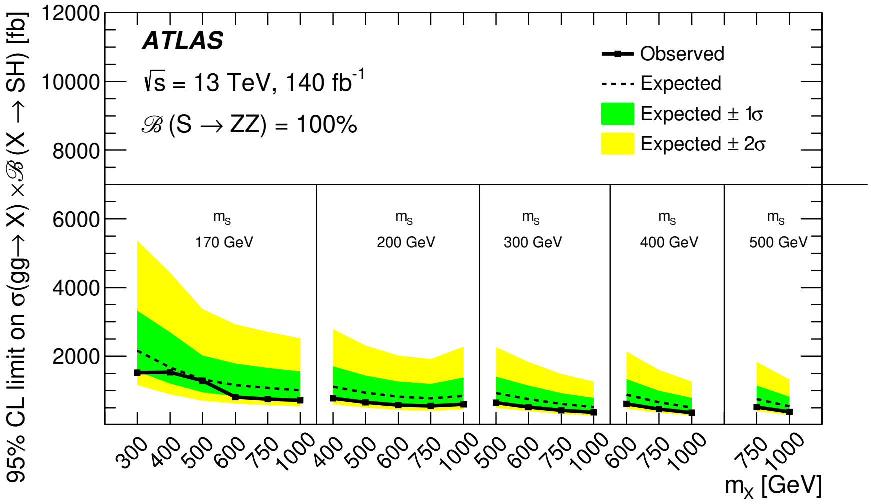

Figure 8. Observed (solid line) and expected (dashed line) 95% CL upper limits on $\sigma(gg \to X) \times \mathscr{B}(X \to SH)$ as a function of m_X and m_S, under the assumption of $\mathscr{B}(S \to ZZ) = 100\%$. The green and yellow shaded areas indicate the ± 1 and ± 2 standard deviations around the expected limit.

These results are comparable to the $X \to SH \to VV\tau\tau$ [15] search, which observes an upper limit on the production cross-section from 540 fb to 72 fb, assuming SM-like $\mathscr{B}(S \to WW/ZZ)$. Under the $\mathscr{B}(S \to WW) = 100\%$ and $\mathscr{B}(S \to ZZ) = 100\%$ scenarios, the upper limits on the production cross-section and decay branching ratio are in the ranges 26–3 fb and 33–6 fb, respectively. By correcting by the $\mathscr{B}(H \to \tau\tau)$, these results can be expressed in upper limits on the $X \to SH$ production cross-section, and compared to those obtained by this analysis. These upper limits are set in the ranges 410–47 fb and 520–95 fb for $\mathscr{B}(S \to WW) = 100\%$ and $\mathscr{B}(S \to ZZ) = 100\%$, respectively.

8 Conclusion

This paper presents the first search for the $X \to SH \to VV\gamma\gamma$ process by selecting events with a pair of photons accompanied by one or two leptons (electrons or muons). The analysis is based on 140 fb^{-1} of proton-proton collision data at $\sqrt{s} = 13$ TeV recorded with the ATLAS detector at the LHC. The $X \to SH \to VV\gamma\gamma$ signal is searched for over the $300 \leq m_X \leq 1000$ GeV and $170 \leq m_S \leq 500$ GeV mass ranges, probing lower m_X values than the ATLAS $SH \to VV\tau\tau$ search, and complementing the ATLAS $X \to SH \to bb\gamma\gamma$ search by testing a different S-boson decay mode.

No excess of events above the expected SM background is observed and 95% CL upper limits are set on the cross-section times branching ratio, $\sigma(gg \to X) \times \mathscr{B}(X \to SH)$, under different assumptions for the $S \to WW/ZZ$ branching ratios. The observed (expected) upper limits lie in the range of 530 – 120 fb (800 – 170 fb) under the assumption that $\mathscr{B}(S \to WW/ZZ)$ corresponding to those the SM Higgs boson would have at the mass of the S particle. The corresponding observed (expected) upper limits on the cross-section are in the range of 470 – 91 fb (610 – 120 fb) under the assumption of $\mathscr{B}(S \to WW) = 100\%$. Alternatively, under the assumption of $\mathscr{B}(S \to ZZ) = 100\%$, the observed (expected) limits are in the range of 1530 – 360 fb (2160 – 510 fb).

Acknowledgments

We thank CERN for the very successful operation of the LHC and its injectors, as well as the support staff at CERN and at our institutions worldwide without whom ATLAS could not be operated efficiently.

The crucial computing support from all WLCG partners is acknowledged gratefully, in particular from CERN, the ATLAS Tier-1 facilities at TRIUMF/SFU (Canada), NDGF (Denmark, Norway, Sweden), CC-IN2P3 (France), KIT/GridKA (Germany), INFN-CNAF (Italy), NL-T1 (Netherlands), PIC (Spain), RAL (UK) and BNL (USA), the Tier-2 facilities worldwide and large non-WLCG resource providers. Major contributors of computing resources are listed in ref. [109].

We gratefully acknowledge the support of ANPCyT, Argentina; YerPhI, Armenia; ARC, Australia; BMWFW and FWF, Austria; ANAS, Azerbaijan; CNPq and FAPESP, Brazil; NSERC, NRC and CFI, Canada; CERN; ANID, Chile; CAS, MOST and NSFC, China; Minciencias, Colombia; MEYS CR, Czech Republic; DNRF and DNSRC, Denmark; IN2P3-CNRS and CEA-DRF/IRFU, France; SRNSFG, Georgia; BMBF, HGF and MPG, Germany; GSRI, Greece; RGC and Hong Kong SAR, China; ISF and Benoziyo Center, Israel; INFN, Italy; MEXT and JSPS, Japan; CNRST, Morocco; NWO, Netherlands; RCN, Norway; MNiSW, Poland; FCT, Portugal; MNE/IFA, Romania; MESTD, Serbia; MSSR, Slovakia; ARIS and MVZI, Slovenia; DSI/NRF, South Africa; MICIU/AEI, Spain; SRC and Wallenberg Foundation, Sweden; SERI, SNSF and Cantons of Bern and Geneva, Switzerland; NSTC, Taipei; TENMAK, Türkiye; STFC/UKRI, United Kingdom; DOE and NSF, United States of America.

Individual groups and members have received support from BCKDF, CANARIE, CRC and DRAC, Canada; CERN-CZ, FORTE and PRIMUS, Czech Republic; COST, ERC, ERDF, Horizon 2020, ICSC-NextGenerationEU and Marie Skłodowska-Curie Actions, European Union; Investissements d'Avenir Labex, Investissements d'Avenir Idex and ANR, France; DFG and AvH Foundation, Germany; Herakleitos, Thales and Aristeia programmes co-financed by EU-ESF and the Greek NSRF, Greece; BSF-NSF and MINERVA, Israel; NCN and NAWA, Poland; La Caixa Banking Foundation, CERCA Programme Generalitat de Catalunya and PROMETEO and GenT Programmes Generalitat Valenciana, Spain; Göran Gustafssons Stiftelse, Sweden; The Royal Society and Leverhulme Trust, United Kingdom.

In addition, individual members wish to acknowledge support from Armenia: Yerevan Physics Institute (FAPERJ); CERN: European Organization for Nuclear Research (CERN PJAS); Chile: Agencia Nacional de Investigación y Desarrollo (FONDECYT 1230812, FONDECYT 1230987, FONDECYT 1240864); China: Chinese Ministry of Science and Technology (MOST-2023YFA1605700), National Natural Science Foundation of China (NSFC — 12175119, NSFC 12275265, NSFC-12075060); Czech Republic: Czech Science Foundation (GACR — 24-11373S), Ministry of Education Youth and Sports (FORTE CZ.02.01.01/00/22_008/0004632), PRIMUS Research Programme (PRIMUS/21/SCI/017); EU: H2020 European Research Council (ERC — 101002463); European Union: European Research Council (ERC — 948254, ERC 101089007), Horizon 2020 Framework Programme (MUCCA — CHIST-ERA-19-XAI-00), European Union, Future Artificial Intelligence Research (FAIR-NextGenerationEU PE00000013), Italian Center for High Performance Com-

JHEP10(2024)104

puting, Big Data and Quantum Computing (ICSC, NextGenerationEU); France: Agence Nationale de la Recherche (ANR-20-CE31-0013, ANR-21-CE31-0013, ANR-21-CE31-0022, ANR-22-EDIR-0002), Investissements d'Avenir Labex (ANR-11-LABX-0012); Germany: Baden-Württemberg Stiftung (BW Stiftung-Postdoc Eliteprogramme), Deutsche Forschungsgemeinschaft (DFG — 469666862, DFG — CR 312/5-2); Italy: Istituto Nazionale di Fisica Nucleare (ICSC, NextGenerationEU), Ministero dell'Università e della Ricerca (PRIN — 20223N7F8K — PNRR M4.C2.1.1); Japan: Japan Society for the Promotion of Science (JSPS KAKENHI JP22H01227, JSPS KAKENHI JP22H04944, JSPS KAKENHI JP22KK0227, JSPS KAKENHI JP23KK0245); Netherlands: Netherlands Organisation for Scientific Research (NWO Veni 2020 — VI.Veni.202.179); Norway: Research Council of Norway (RCN-314472); Poland: Ministry of Science and Higher Education (IDUB AGH, POB8, D4 no 9722), Polish National Agency for Academic Exchange (PPN/PPO/2020/1/00002/U/00001), Polish National Science Centre (NCN 2021/42/E/ST2/00350, NCN OPUS nr 2022/47/B/ST2/03059, NCN UMO-2019/34/E/ST2/00393, UMO-2020/37/B/ST2/01043, UMO-2021/40/C/ST2/00187, UMO-2022/47/O/ST2/00148, UMO-2023/49/B/ST2/04085); Slovenia: Slovenian Research Agency (ARIS grant J1-3010); Spain: Generalitat Valenciana (Artemisa, FEDER, IDIFEDER/2018/048), Ministry of Science and Innovation (MCIN & NextGenEU PCI2022-135018-2, MICIN & FEDER PID2021-125273NB, RYC2019-028510-I, RYC2020-030254-I, RYC2021-031273-I, RYC2022-038164-I), PROMETEO and GenT Programmes Generalitat Valenciana (CIDEGENT/2019/027); Sweden: Swedish Research Council (Swedish Research Council 2023-04654, VR 2018-00482, VR 2022-03845, VR 2022-04683, VR 2023-03403, VR grant 2021-03651), Knut and Alice Wallenberg Foundation (KAW 2018.0157, KAW 2018.0458, KAW 2019.0447, KAW 2022.0358); Switzerland: Swiss National Science Foundation (SNSF — PCEFP2_194658); United Kingdom: Leverhulme Trust (Leverhulme Trust RPG-2020-004), Royal Society (NIF-R1-231091); United States of America: U.S. Department of Energy (ECA DE-AC02-76SF00515), Neubauer Family Foundation.

References

[1] ATLAS collaboration, *The ATLAS Experiment at the CERN Large Hadron Collider*, 2008 *JINST* **3** S08003 [INSPIRE].

[2] CMS collaboration, *The CMS Experiment at the CERN LHC*, 2008 *JINST* **3** S08004 [INSPIRE].

[3] ATLAS collaboration, *Observation of a new particle in the search for the Standard Model Higgs boson with the ATLAS detector at the LHC*, *Phys. Lett. B* **716** (2012) 1 [arXiv:1207.7214] [INSPIRE].

[4] CMS collaboration, *Observation of a New Boson at a Mass of 125 GeV with the CMS Experiment at the LHC*, *Phys. Lett. B* **716** (2012) 30 [arXiv:1207.7235] [INSPIRE].

[5] ATLAS collaboration, *A detailed map of Higgs boson interactions by the ATLAS experiment ten years after the discovery*, *Nature* **607** (2022) 52 [*Erratum ibid.* **612** (2022) E24] [arXiv:2207.00092] [INSPIRE].

JHEP10(2024)104

[6] CMS collaboration, *A portrait of the Higgs boson by the CMS experiment ten years after the discovery.*, *Nature* **607** (2022) 60 [arXiv:2207.00043] [INSPIRE].

[7] U. Ellwanger, C. Hugonie and A.M. Teixeira, *The Next-to-Minimal Supersymmetric Standard Model*, *Phys. Rept.* **496** (2010) 1 [arXiv:0910.1785] [INSPIRE].

[8] M. Maniatis, *The Next-to-Minimal Supersymmetric extension of the Standard Model reviewed*, *Int. J. Mod. Phys. A* **25** (2010) 3505 [arXiv:0906.0777] [INSPIRE].

[9] T. Robens, T. Stefaniak and J. Wittbrodt, *Two-real-scalar-singlet extension of the SM: LHC phenomenology and benchmark scenarios*, *Eur. Phys. J. C* **80** (2020) 151 [arXiv:1908.08554] [INSPIRE].

[10] T. Robens, *Two-Real-Singlet-Model Benchmark Planes*, *Symmetry* **15** (2023) 27 [arXiv:2209.10996] [INSPIRE].

[11] G.C. Branco et al., *Theory and phenomenology of two-Higgs-doublet models*, *Phys. Rept.* **516** (2012) 1 [arXiv:1106.0034] [INSPIRE].

[12] S. Baum and N.R. Shah, *Two Higgs Doublets and a Complex Singlet: Disentangling the Decay Topologies and Associated Phenomenology*, *JHEP* **12** (2018) 044 [arXiv:1808.02667] [INSPIRE].

[13] ATLAS collaboration, *Search for Higgs boson pair production in the $WW^{(*)}WW^{(*)}$ decay channel using ATLAS data recorded at $\sqrt{s} = 13$ TeV*, *JHEP* **05** (2019) 124 [arXiv:1811.11028] [INSPIRE].

[14] ATLAS collaboration, *Search for a resonance decaying into a scalar particle and a Higgs boson in the final state with two bottom quarks and two photons in proton-proton collisions at a center of mass energy of 13 TeV with the ATLAS detector*, arXiv:2404.12915 [INSPIRE].

[15] ATLAS collaboration, *Search for a new heavy scalar particle decaying into a Higgs boson and a new scalar singlet in final states with one or two light leptons and a pair of τ-leptons with the ATLAS detector*, *JHEP* **10** (2023) 009 [arXiv:2307.11120] [INSPIRE].

[16] CMS collaboration, *Search for a new resonance decaying into two spin-0 bosons in a final state with two photons and two bottom quarks in proton-proton collisions at $\sqrt{s} = 13$ TeV*, *JHEP* **05** (2024) 316 [arXiv:2310.01643] [INSPIRE].

[17] CMS collaboration, *Search for a heavy Higgs boson decaying into two lighter Higgs bosons in the $\tau\tau bb$ final state at 13 TeV*, *JHEP* **11** (2021) 057 [arXiv:2106.10361] [INSPIRE].

[18] CMS collaboration, *Search for a massive scalar resonance decaying to a light scalar and a Higgs boson in the four b quarks final state with boosted topology*, *Phys. Lett. B* **842** (2023) 137392 [arXiv:2204.12413] [INSPIRE].

[19] LHC Higgs Cross Section Working Group collaboration, *Handbook of LHC Higgs Cross Sections: 4. Deciphering the Nature of the Higgs Sector*, arXiv:1610.07922 [DOI:10.23731/CYRM-2017-002] [INSPIRE].

[20] ATLAS collaboration, *Measurements of the Higgs boson inclusive and differential fiducial cross-sections in the diphoton decay channel with pp collisions at $\sqrt{s} = 13$ TeV with the ATLAS detector*, *JHEP* **08** (2022) 027 [arXiv:2202.00487] [INSPIRE].

[21] ATLAS collaboration, *ATLAS Insertable B-Layer Technical Design Report*, CERN-LHCC-2010-013 (2010).

[22] ATLAS IBL collaboration, *Production and Integration of the ATLAS Insertable B-Layer*, 2018 *JINST* **13** T05008 [arXiv:1803.00844] [INSPIRE].

JHEP10(2024)104

[23] G. Avoni et al., *The new LUCID-2 detector for luminosity measurement and monitoring in ATLAS*, 2018 *JINST* **13** P07017 [INSPIRE].

[24] ATLAS collaboration, *Performance of the ATLAS Trigger System in 2015*, *Eur. Phys. J. C* **77** (2017) 317 [arXiv:1611.09661] [INSPIRE].

[25] ATLAS collaboration, *Software and computing for Run 3 of the ATLAS experiment at the LHC*, arXiv:2404.06335 [INSPIRE].

[26] ATLAS collaboration, *Luminosity determination in pp collisions at* $\sqrt{s} = 13$ *TeV using the ATLAS detector at the LHC*, *Eur. Phys. J. C* **83** (2023) 982 [arXiv:2212.09379] [INSPIRE].

[27] ATLAS collaboration, *ATLAS data quality operations and performance for 2015–2018 data-taking*, 2020 *JINST* **15** P04003 [arXiv:1911.04632] [INSPIRE].

[28] ATLAS collaboration, *Performance of electron and photon triggers in ATLAS during LHC Run 2*, *Eur. Phys. J. C* **80** (2020) 47 [arXiv:1909.00761] [INSPIRE].

[29] T. Sjöstrand et al., *An introduction to PYTHIA 8.2*, *Comput. Phys. Commun.* **191** (2015) 159 [arXiv:1410.3012] [INSPIRE].

[30] ATLAS collaboration *ATLAS Pythia 8 tunes to 7 TeV data*, ATL-PHYS-PUB-2014-021, CERN, Geneva (2014).

[31] R.D. Ball et al., *Parton distributions with LHC data*, *Nucl. Phys. B* **867** (2013) 244 [arXiv:1207.1303] [INSPIRE].

[32] K. Hamilton, P. Nason, E. Re and G. Zanderighi, *NNLOPS simulation of Higgs boson production*, *JHEP* **10** (2013) 222 [arXiv:1309.0017] [INSPIRE].

[33] K. Hamilton, P. Nason and G. Zanderighi, *Finite quark-mass effects in the NNLOPS POWHEG+MiNLO Higgs generator*, *JHEP* **05** (2015) 140 [arXiv:1501.04637] [INSPIRE].

[34] S. Alioli, P. Nason, C. Oleari and E. Re, *A general framework for implementing NLO calculations in shower Monte Carlo programs: the POWHEG BOX*, *JHEP* **06** (2010) 043 [arXiv:1002.2581] [INSPIRE].

[35] P. Nason, *A New method for combining NLO QCD with shower Monte Carlo algorithms*, *JHEP* **11** (2004) 040 [hep-ph/0409146] [INSPIRE].

[36] S. Frixione, P. Nason and C. Oleari, *Matching NLO QCD computations with Parton Shower simulations: the POWHEG method*, *JHEP* **11** (2007) 070 [arXiv:0709.2092] [INSPIRE].

[37] K. Hamilton, P. Nason and G. Zanderighi, *MINLO: Multi-Scale Improved NLO*, *JHEP* **10** (2012) 155 [arXiv:1206.3572] [INSPIRE].

[38] J.M. Campbell et al., *NLO Higgs Boson Production Plus One and Two Jets Using the POWHEG BOX, MadGraph4 and MCFM*, *JHEP* **07** (2012) 092 [arXiv:1202.5475] [INSPIRE].

[39] K. Hamilton, P. Nason, C. Oleari and G. Zanderighi, *Merging H/W/Z + 0 and 1 jet at NLO with no merging scale: a path to parton shower + NNLO matching*, *JHEP* **05** (2013) 082 [arXiv:1212.4504] [INSPIRE].

[40] S. Catani and M. Grazzini, *An NNLO subtraction formalism in hadron collisions and its application to Higgs boson production at the LHC*, *Phys. Rev. Lett.* **98** (2007) 222002 [hep-ph/0703012] [INSPIRE].

[41] J. Butterworth et al., *PDF4LHC recommendations for LHC Run II*, *J. Phys. G* **43** (2016) 023001 [arXiv:1510.03865] [INSPIRE].

[42] ATLAS collaboration, *Measurement of the Z/γ^* boson transverse momentum distribution in pp collisions at $\sqrt{s} = 7$ TeV with the ATLAS detector*, JHEP **09** (2014) 145 [arXiv:1406.3660] [INSPIRE].

[43] D.J. Lange, *The EvtGen particle decay simulation package*, Nucl. Instrum. Meth. A **462** (2001) 152 [INSPIRE].

[44] C. Anastasiou et al., *High precision determination of the gluon fusion Higgs boson cross-section at the LHC*, JHEP **05** (2016) 058 [arXiv:1602.00695] [INSPIRE].

[45] C. Anastasiou et al., *Higgs Boson Gluon-Fusion Production in QCD at Three Loops*, Phys. Rev. Lett. **114** (2015) 212001 [arXiv:1503.06056] [INSPIRE].

[46] F. Dulat, A. Lazopoulos and B. Mistlberger, *iHixs 2 — Inclusive Higgs cross sections*, Comput. Phys. Commun. **233** (2018) 243 [arXiv:1802.00827] [INSPIRE].

[47] R.V. Harlander and K.J. Ozeren, *Finite top mass effects for hadronic Higgs production at next-to-next-to-leading order*, JHEP **11** (2009) 088 [arXiv:0909.3420] [INSPIRE].

[48] R.V. Harlander and K.J. Ozeren, *Top mass effects in Higgs production at next-to-next-to-leading order QCD: Virtual corrections*, Phys. Lett. B **679** (2009) 467 [arXiv:0907.2997] [INSPIRE].

[49] R.V. Harlander, H. Mantler, S. Marzani and K.J. Ozeren, *Higgs production in gluon fusion at next-to-next-to-leading order QCD for finite top mass*, Eur. Phys. J. C **66** (2010) 359 [arXiv:0912.2104] [INSPIRE].

[50] A. Pak, M. Rogal and M. Steinhauser, *Finite top quark mass effects in NNLO Higgs boson production at LHC*, JHEP **02** (2010) 025 [arXiv:0911.4662] [INSPIRE].

[51] S. Actis, G. Passarino, C. Sturm and S. Uccirati, *NLO Electroweak Corrections to Higgs Boson Production at Hadron Colliders*, Phys. Lett. B **670** (2008) 12 [arXiv:0809.1301] [INSPIRE].

[52] S. Actis, G. Passarino, C. Sturm and S. Uccirati, *NNLO Computational Techniques: The Cases $H \to \gamma\gamma$ and $H \to gg$*, Nucl. Phys. B **811** (2009) 182 [arXiv:0809.3667] [INSPIRE].

[53] M. Bonetti, K. Melnikov and L. Tancredi, *Higher order corrections to mixed QCD-EW contributions to Higgs boson production in gluon fusion*, Phys. Rev. D **97** (2018) 056017 [*Erratum ibid.* **97** (2018) 099906] [arXiv:1801.10403] [INSPIRE].

[54] M. Ciccolini, A. Denner and S. Dittmaier, *Strong and electroweak corrections to the production of Higgs + 2jets via weak interactions at the LHC*, Phys. Rev. Lett. **99** (2007) 161803 [arXiv:0707.0381] [INSPIRE].

[55] M. Ciccolini, A. Denner and S. Dittmaier, *Electroweak and QCD corrections to Higgs production via vector-boson fusion at the LHC*, Phys. Rev. D **77** (2008) 013002 [arXiv:0710.4749] [INSPIRE].

[56] P. Bolzoni, F. Maltoni, S.-O. Moch and M. Zaro, *Higgs production via vector-boson fusion at NNLO in QCD*, Phys. Rev. Lett. **105** (2010) 011801 [arXiv:1003.4451] [INSPIRE].

[57] G. Luisoni, P. Nason, C. Oleari and F. Tramontano, *$HW^{\pm}/HZ + 0$ and 1 jet at NLO with the POWHEG BOX interfaced to GoSam and their merging within MiNLO*, JHEP **10** (2013) 083 [arXiv:1306.2542] [INSPIRE].

[58] M.L. Ciccolini, S. Dittmaier and M. Kramer, *Electroweak radiative corrections to associated WH and ZH production at hadron colliders*, Phys. Rev. D **68** (2003) 073003 [hep-ph/0306234] [INSPIRE].

[59] O. Brein, A. Djouadi and R. Harlander, *NNLO QCD corrections to the Higgs-strahlung processes at hadron colliders*, Phys. Lett. B **579** (2004) 149 [hep-ph/0307206] [INSPIRE].

JHEP10(2024)104

[60] O. Brein, R. Harlander, M. Wiesemann and T. Zirke, *Top-Quark Mediated Effects in Hadronic Higgs-Strahlung*, *Eur. Phys. J. C* **72** (2012) 1868 [arXiv:1111.0761] [INSPIRE].

[61] L. Altenkamp et al., *Gluon-induced Higgs-strahlung at next-to-leading order QCD*, *JHEP* **02** (2013) 078 [arXiv:1211.5015] [INSPIRE].

[62] A. Denner, S. Dittmaier, S. Kallweit and A. Mück, *HAWK 2.0: A Monte Carlo program for Higgs production in vector-boson fusion and Higgs strahlung at hadron colliders*, *Comput. Phys. Commun.* **195** (2015) 161 [arXiv:1412.5390] [INSPIRE].

[63] O. Brein, R.V. Harlander and T.J.E. Zirke, *vh@nnlo — Higgs Strahlung at hadron colliders*, *Comput. Phys. Commun.* **184** (2013) 998 [arXiv:1210.5347] [INSPIRE].

[64] R.V. Harlander, A. Kulesza, V. Theeuwes and T. Zirke, *Soft gluon resummation for gluon-induced Higgs Strahlung*, *JHEP* **11** (2014) 082 [arXiv:1410.0217] [INSPIRE].

[65] NNPDF collaboration, *Parton distributions for the LHC Run II*, *JHEP* **04** (2015) 040 [arXiv:1410.8849] [INSPIRE].

[66] J. Alwall et al., *The automated computation of tree-level and next-to-leading order differential cross sections, and their matching to parton shower simulations*, *JHEP* **07** (2014) 079 [arXiv:1405.0301] [INSPIRE].

[67] A. Djouadi, J. Kalinowski and M. Spira, *HDECAY: A Program for Higgs boson decays in the standard model and its supersymmetric extension*, *Comput. Phys. Commun.* **108** (1998) 56 [hep-ph/9704448] [INSPIRE].

[68] M. Spira, *QCD effects in Higgs physics*, *Fortsch. Phys.* **46** (1998) 203 [hep-ph/9705337] [INSPIRE].

[69] A. Djouadi, M.M. Muhlleitner and M. Spira, *Decays of supersymmetric particles: The Program SUSY-HIT (SUspect-SdecaY-Hdecay-InTerface)*, *Acta Phys. Polon. B* **38** (2007) 635 [hep-ph/0609292] [INSPIRE].

[70] A. Bredenstein, A. Denner, S. Dittmaier and M.M. Weber, *Radiative corrections to the semileptonic and hadronic Higgs-boson decays $H \to WW/ZZ \to 4$ fermions*, *JHEP* **02** (2007) 080 [hep-ph/0611234] [INSPIRE].

[71] A. Bredenstein, A. Denner, S. Dittmaier and M.M. Weber, *Precise predictions for the Higgs-boson decay $H \to WW/ZZ \to 4$ leptons*, *Phys. Rev. D* **74** (2006) 013004 [hep-ph/0604011] [INSPIRE].

[72] A. Bredenstein, A. Denner, S. Dittmaier and M.M. Weber, *Precision calculations for the Higgs decays $H \to ZZ/WW \to 4$ leptons*, *Nucl. Phys. B Proc. Suppl.* **160** (2006) 131 [hep-ph/0607060] [INSPIRE].

[73] SHERPA collaboration, *Event Generation with Sherpa 2.2*, *SciPost Phys.* **7** (2019) 034 [arXiv:1905.09127] [INSPIRE].

[74] T. Gleisberg and S. Hoeche, *Comix, a new matrix element generator*, *JHEP* **12** (2008) 039 [arXiv:0808.3674] [INSPIRE].

[75] F. Cascioli, P. Maierhofer and S. Pozzorini, *Scattering Amplitudes with Open Loops*, *Phys. Rev. Lett.* **108** (2012) 111601 [arXiv:1111.5206] [INSPIRE].

[76] A. Denner, S. Dittmaier and L. Hofer, *Collier: a fortran-based Complex One-Loop LIbrary in Extended Regularizations*, *Comput. Phys. Commun.* **212** (2017) 220 [arXiv:1604.06792] [INSPIRE].

[77] S. Schumann and F. Krauss, *A Parton shower algorithm based on Catani-Seymour dipole factorisation*, *JHEP* **03** (2008) 038 [arXiv:0709.1027] [INSPIRE].

[78] S. Catani, F. Krauss, R. Kuhn and B.R. Webber, *QCD matrix elements + parton showers*, *JHEP* **11** (2001) 063 [hep-ph/0109231] [INSPIRE].

[79] S. Hoeche, F. Krauss, S. Schumann and F. Siegert, *QCD matrix elements and truncated showers*, *JHEP* **05** (2009) 053 [arXiv:0903.1219] [INSPIRE].

[80] S. Hoeche, F. Krauss, M. Schonherr and F. Siegert, *A critical appraisal of NLO+PS matching methods*, *JHEP* **09** (2012) 049 [arXiv:1111.1220] [INSPIRE].

[81] S. Hoeche, F. Krauss, M. Schonherr and F. Siegert, *QCD matrix elements + parton showers: The NLO case*, *JHEP* **04** (2013) 027 [arXiv:1207.5030] [INSPIRE].

[82] GEANT4 collaboration, *GEANT4 — a simulation toolkit*, *Nucl. Instrum. Meth. A* **506** (2003) 250 [INSPIRE].

[83] ATLAS collaboration, *The ATLAS Simulation Infrastructure*, *Eur. Phys. J. C* **70** (2010) 823 [arXiv:1005.4568] [INSPIRE].

[84] C. ATLAS et al., *The simulation principle and performance of the ATLAS fast calorimeter simulation FastCaloSim*, ATL-PHYS-PUB-2010-013, CERN, Geneva (2010).

[85] T. Sjostrand, S. Mrenna and P.Z. Skands, *A Brief Introduction to PYTHIA 8.1*, *Comput. Phys. Commun.* **178** (2008) 852 [arXiv:0710.3820] [INSPIRE].

[86] ATLAS collaboration, *The Pythia 8 A3 tune description of ATLAS minimum bias and inelastic measurements incorporating the Donnachie-Landshoff diffractive model*, ATL-PHYS-PUB-2016-017, CERN, Geneva (2016).

[87] ATLAS collaboration, *Measurement of Higgs boson production in the diphoton decay channel in pp collisions at center-of-mass energies of 7 and 8 TeV with the ATLAS detector*, *Phys. Rev. D* **90** (2014) 112015 [arXiv:1408.7084] [INSPIRE].

[88] ATLAS collaboration, *Electron and photon performance measurements with the ATLAS detector using the 2015–2017 LHC proton-proton collision data*, 2019 *JINST* **14** P12006 [arXiv:1908.00005] [INSPIRE].

[89] ATLAS collaboration, *Muon reconstruction and identification efficiency in ATLAS using the full Run 2 pp collision data set at* $\sqrt{s} = 13$ *TeV*, *Eur. Phys. J. C* **81** (2021) 578 [arXiv:2012.00578] [INSPIRE].

[90] ATLAS collaboration, *Jet reconstruction and performance using particle flow with the ATLAS Detector*, *Eur. Phys. J. C* **77** (2017) 466 [arXiv:1703.10485] [INSPIRE].

[91] ATLAS collaboration, *Topological cell clustering in the ATLAS calorimeters and its performance in LHC Run 1*, *Eur. Phys. J. C* **77** (2017) 490 [arXiv:1603.02934] [INSPIRE].

[92] M. Cacciari, G.P. Salam and G. Soyez, *FastJet User Manual*, *Eur. Phys. J. C* **72** (2012) 1896 [arXiv:1111.6097] [INSPIRE].

[93] M. Cacciari, G.P. Salam and G. Soyez, *The anti-*k_t *jet clustering algorithm*, *JHEP* **04** (2008) 063 [arXiv:0802.1189] [INSPIRE].

[94] ATLAS collaboration, *Jet energy scale and resolution measured in proton-proton collisions at* $\sqrt{s} = 13$ *TeV with the ATLAS detector*, *Eur. Phys. J. C* **81** (2021) 689 [arXiv:2007.02645] [INSPIRE].

JHEP10(2024)104

[95] ATLAS collaboration, *Performance of pile-up mitigation techniques for jets in pp collisions at* $\sqrt{s} = 8$ *TeV using the ATLAS detector*, *Eur. Phys. J. C* **76** (2016) 581 [arXiv:1510.03823] [INSPIRE].

[96] ATLAS collaboration, *ATLAS flavour-tagging algorithms for the LHC Run 2 pp collision dataset*, *Eur. Phys. J. C* **83** (2023) 681 [arXiv:2211.16345] [INSPIRE].

[97] ATLAS collaboration, *The performance of missing transverse momentum reconstruction and its significance with the ATLAS detector using 140 fb*$^{-1}$ *of* $\sqrt{s} = 13$ *TeV pp collisions*, arXiv:2402.05858 [INSPIRE].

[98] P. Baldi et al., *Parameterized neural networks for high-energy physics*, *Eur. Phys. J. C* **76** (2016) 235 [arXiv:1601.07913] [INSPIRE].

[99] ATLAS collaboration, *Recommendations for the Modeling of Smooth Backgrounds*, ATL-PHYS-PUB-2020-028, CERN, Geneva (2020).

[100] ATLAS collaboration, *Electron and photon efficiencies in LHC Run 2 with the ATLAS experiment*, *JHEP* **05** (2024) 162 [arXiv:2308.13362] [INSPIRE].

[101] ATLAS collaboration, *ATLAS b-jet identification performance and efficiency measurement with* $t\bar{t}$ *events in pp collisions at* $\sqrt{s} = 13$ *TeV*, *Eur. Phys. J. C* **79** (2019) 970 [arXiv:1907.05120] [INSPIRE].

[102] ATLAS collaboration, *Measurement of the c-jet mistagging efficiency in* $t\bar{t}$ *events using pp collision data at* $\sqrt{s} = 13$ *TeV collected with the ATLAS detector*, *Eur. Phys. J. C* **82** (2022) 95 [arXiv:2109.10627] [INSPIRE].

[103] ATLAS collaboration, *Calibration of the light-flavour jet mistagging efficiency of the b-tagging algorithms with Z+jets events using 139 fb*$^{-1}$ *of ATLAS proton-proton collision data at* $\sqrt{s} = 13$ *TeV*, *Eur. Phys. J. C* **83** (2023) 728 [arXiv:2301.06319] [INSPIRE].

[104] W. Verkerke and D.P. Kirkby, *The RooFit toolkit for data modeling*, *eConf C* **0303241** (2003) MOLT007 [physics/0306116] [INSPIRE].

[105] L. Moneta et al., *The RooStats Project*, *PoS* **ACAT2010** (2010) 057 [arXiv:1009.1003] [INSPIRE].

[106] G. Cowan, K. Cranmer, E. Gross and O. Vitells, *Asymptotic formulae for likelihood-based tests of new physics*, *Eur. Phys. J. C* **71** (2011) 1554 [*Erratum ibid.* **73** (2013) 2501] [arXiv:1007.1727] [INSPIRE].

[107] A.L. Read, *Presentation of search results: The* CL_s *technique*, *J. Phys. G* **28** (2002) 2693 [INSPIRE].

[108] T. Junk, *Confidence level computation for combining searches with small statistics*, *Nucl. Instrum. Meth. A* **434** (1999) 435 [hep-ex/9902006] [INSPIRE].

[109] ATLAS collaboration, *ATLAS Computing Acknowledgements*, ATL-SOFT-PUB-2023-001, CERN, Geneva (2023).

The ATLAS collaboration

G. Aad[104], E. Aakvaag[17], B. Abbott[123], S. Abdelhameed[119a], K. Abeling[56], N.J. Abicht[50], S.H. Abidi[30], M. Aboelela[45], A. Aboulhorma[36e], H. Abramowicz[154], H. Abreu[153], Y. Abulaiti[120], B.S. Acharya[70a,70b,l], A. Ackermann[64a], C. Adam Bourdarios[4], L. Adamczyk[87a], S.V. Addepalli[27], M.J. Addison[103], J. Adelman[118], A. Adiguzel[22c], T. Adye[137], A.A. Affolder[139], Y. Afik[40], M.N. Agaras[13], J. Agarwala[74a,74b], A. Aggarwal[102], C. Agheorghiesei[28c], F. Ahmadov[39,z], W.S. Ahmed[106], S. Ahuja[97], X. Ai[63e], G. Aielli[77a,77b], A. Aikot[166], M. Ait Tamlihat[36e], B. Aitbenchikh[36a], M. Akbiyik[102], T.P.A. Åkesson[100], A.V. Akimov[38], D. Akiyama[171], N.N. Akolkar[25], S. Aktas[22a], K. Al Khoury[42], G.L. Alberghi[24b], J. Albert[168], P. Albicocco[54], G.L. Albouy[61], S. Alderweireldt[53], Z.L. Alegria[124], M. Aleksa[37], I.N. Aleksandrov[39], C. Alexa[28b], T. Alexopoulos[10], F. Alfonsi[24b], M. Algren[57], M. Alhroob[170], B. Ali[135], H.M.J. Ali[93], S. Ali[32], S.W. Alibocus[94], M. Aliev[34c], G. Alimonti[72a], W. Alkakhi[56], C. Allaire[67], B.M.M. Allbrooke[149], J.F. Allen[53], C.A. Allendes Flores[140f], P.P. Allport[21], A. Aloisio[73a,73b], F. Alonso[92], C. Alpigiani[141], Z.M.K. Alsolami[93], M. Alvarez Estevez[101], A. Alvarez Fernandez[102], M. Alves Cardoso[57], M.G. Alviggi[73a,73b], M. Aly[103], Y. Amaral Coutinho[84b], A. Ambler[106], C. Amelung[37], M. Amerl[103], C.G. Ames[111], D. Amidei[108], B. Amini[55], K.J. Amirie[158], S.P. Amor Dos Santos[133a], K.R. Amos[166], S. An[85], V. Ananiev[128], C. Anastopoulos[142], T. Andeen[11], J.K. Anders[37], A.C. Anderson[60], S.Y. Andrean[48a,48b], A. Andreazza[72a,72b], S. Angelidakis[9], A. Angerami[42], A.V. Anisenkov[38], A. Annovi[75a], C. Antel[57], E. Antipov[148], M. Antonelli[54], F. Anulli[76a], M. Aoki[85], T. Aoki[156], M.A. Aparo[149], L. Aperio Bella[49], C. Appelt[19], A. Apyan[27], S.J. Arbiol Val[88], C. Arcangeletti[54], A.T.H. Arce[52], J-F. Arguin[110], S. Argyropoulos[55], J.-H. Arling[49], O. Arnaez[4], H. Arnold[148], G. Artoni[76a,76b], H. Asada[113], K. Asai[121], S. Asai[156], N.A. Asbah[37], R.A. Ashby Pickering[170], K. Assamagan[30], R. Astalos[29a], K.S.V. Astrand[100], S. Atashi[162], R.J. Atkin[34a], M. Atkinson[165], H. Atmani[36f], P.A. Atmasiddha[131], K. Augsten[135], S. Auricchio[73a,73b], A.D. Auriol[21], V.A. Austrup[103], G. Avolio[37], K. Axiotis[57], G. Azuelos[110,ae], D. Babal[29b], H. Bachacou[138], K. Bachas[155,p], A. Bachiu[35], F. Backman[48a,48b], A. Badea[40], T.M. Baer[108], P. Bagnaia[76a,76b], M. Bahmani[19], D. Bahner[55], K. Bai[126], J.T. Baines[137], L. Baines[96], O.K. Baker[175], E. Bakos[16], D. Bakshi Gupta[8], L.E. Balabram Filho[84b], V. Balakrishnan[123], R. Balasubramanian[117], E.M. Baldin[38], P. Balek[87a], E. Ballabene[24b,24a], F. Balli[138], L.M. Baltes[64a], W.K. Balunas[33], J. Balz[102], I. Bamwidhi[119b], E. Banas[88], M. Bandieramonte[132], A. Bandyopadhyay[25], S. Bansal[25], L. Barak[154], M. Barakat[49], E.L. Barberio[107], D. Barberis[58b,58a], M. Barbero[104], M.Z. Barel[117], T. Barillari[112], M-S. Barisits[37], T. Barklow[146], P. Baron[125], D.A. Baron Moreno[103], A. Baroncelli[63a], A.J. Barr[129], J.D. Barr[98], F. Barreiro[101], J. Barreiro Guimarães da Costa[14], U. Barron[154], M.G. Barros Teixeira[133a], S. Barsov[38], F. Bartels[64a], R. Bartoldus[146], A.E. Barton[93], P. Bartos[29a], A. Basan[102], M. Baselga[50], A. Bassalat[67,b], M.J. Basso[159a], S. Bataju[45], R. Bate[167], R.L. Bates[60], S. Batlamous[101], B. Batool[144], M. Battaglia[139], D. Battulga[19], M. Bauce[76a,76b], M. Bauer[80], P. Bauer[25], L.T. Bazzano Hurrell[31], J.B. Beacham[52], T. Beau[130], J.Y. Beaucamp[92], P.H. Beauchemin[161], P. Bechtle[25], H.P. Beck[20,o], K. Becker[170], A.J. Beddall[83], V.A. Bednyakov[39], C.P. Bee[148], L.J. Beemster[16],

JHEP10(2024)104

T.A. Beermann[37], M. Begalli[84d], M. Begel[30], A. Behera[148], J.K. Behr[49], J.F. Beirer[37], F. Beisiegel[25], M. Belfkir[119b], G. Bella[154], L. Bellagamba[24b], A. Bellerive[35], P. Bellos[21], K. Beloborodov[38], D. Benchekroun[36a], F. Bendebba[36a], Y. Benhammou[154], K.C. Benkendorfer[62], L. Beresford[49], M. Beretta[54], E. Bergeaas Kuutmann[164], N. Berger[4], B. Bergmann[135], J. Beringer[18a], G. Bernardi[5], C. Bernius[146], F.U. Bernlochner[25], F. Bernon[37,104], A. Berrocal Guardia[13], T. Berry[97], P. Berta[136], A. Berthold[51], S. Bethke[112], A. Betti[76a,76b], A.J. Bevan[96], N.K. Bhalla[55], S. Bhatta[148], D.S. Bhattacharya[169], P. Bhattarai[146], K.D. Bhide[55], V.S. Bhopatkar[124], R.M. Bianchi[132], G. Bianco[24b,24a], O. Biebel[111], R. Bielski[126], M. Biglietti[78a], C.S. Billingsley[45], Y. Bimgdi[36f], M. Bindi[56], A. Bingul[22b], C. Bini[76a,76b], G.A. Bird[33], M. Birman[172], M. Biros[136], S. Biryukov[149], T. Bisanz[50], E. Bisceglie[44b,44a], J.P. Biswal[137], D. Biswas[144], I. Bloch[49], A. Blue[60], U. Blumenschein[96], J. Blumenthal[102], V.S. Bobrovnikov[38], M. Boehler[55], B. Boehm[169], D. Bogavac[37], A.G. Bogdanchikov[38], C. Bohm[48a], V. Boisvert[97], P. Bokan[37], T. Bold[87a], M. Bomben[5], M. Bona[96], M. Boonekamp[138], C.D. Booth[97], A.G. Borbély[60], I.S. Bordulev[38], G. Borissov[93], D. Bortoletto[129], D. Boscherini[24b], M. Bosman[13], J.D. Bossio Sola[37], K. Bouaouda[36a], N. Bouchhar[166], L. Boudet[4], J. Boudreau[132], E.V. Bouhova-Thacker[93], D. Boumediene[41], R. Bouquet[58b,58a], A. Boveia[122], J. Boyd[37], D. Boye[30], I.R. Boyko[39], L. Bozianu[57], J. Bracinik[21], N. Brahimi[4], G. Brandt[174], O. Brandt[33], F. Braren[49], B. Brau[105], J.E. Brau[126], R. Brener[172], L. Brenner[117], R. Brenner[164], S. Bressler[172], G. Brianti[79a,79b], D. Britton[60], D. Britzger[112], I. Brock[25], R. Brock[109], G. Brooijmans[42], E.M. Brooks[159b], E. Brost[30], L.M. Brown[168], L.E. Bruce[62], T.L. Bruckler[129], P.A. Bruckman de Renstrom[88], B. Brüers[49], A. Bruni[24b], G. Bruni[24b], M. Bruschi[24b], N. Bruscino[76a,76b], T. Buanes[17], Q. Buat[141], D. Buchin[112], A.G. Buckley[60], O. Bulekov[38], B.A. Bullard[146], S. Burdin[94], C.D. Burgard[50], A.M. Burger[37], B. Burghgrave[8], O. Burlayenko[55], J. Burleson[165], J.T.P. Burr[33], J.C. Burzynski[145], E.L. Busch[42], V. Büscher[102], P.J. Bussey[60], J.M. Butler[26], C.M. Buttar[60], J.M. Butterworth[98], W. Buttinger[137], C.J. Buxo Vazquez[109], A.R. Buzykaev[38], S. Cabrera Urbán[166], L. Cadamuro[67], D. Caforio[59], H. Cai[132], Y. Cai[14,114c], Y. Cai[114a], V.M.M. Cairo[37], O. Cakir[3a], N. Calace[37], P. Calafiura[18a], G. Calderini[130], P. Calfayan[69], G. Callea[60], L.P. Caloba[84b], D. Calvet[41], S. Calvet[41], M. Calvetti[75a,75b], R. Camacho Toro[130], S. Camarda[37], D. Camarero Munoz[27], P. Camarri[77a,77b], M.T. Camerlingo[73a,73b], D. Cameron[37], C. Camincher[168], M. Campanelli[98], A. Camplani[43], V. Canale[73a,73b], A.C. Canbay[3a], E. Canonero[97], J. Cantero[166], Y. Cao[165], F. Capocasa[27], M. Capua[44b,44a], A. Carbone[72a,72b], R. Cardarelli[77a], J.C.J. Cardenas[8], G. Carducci[44b,44a], T. Carli[37], G. Carlino[73a], J.I. Carlotto[13], B.T. Carlson[132,q], E.M. Carlson[168,159a], J. Carmignani[94], L. Carminati[72a,72b], A. Carnelli[138], M. Carnesale[76a,76b], S. Caron[116], E. Carquin[140f], S. Carrá[72a], G. Carratta[24b,24a], A.M. Carroll[126], T.M. Carter[53], M.P. Casado[13,i], M. Caspar[49], F.L. Castillo[4], L. Castillo Garcia[13], V. Castillo Gimenez[166], N.F. Castro[133a,133e], A. Catinaccio[37], J.R. Catmore[128], T. Cavaliere[4], V. Cavaliere[30], N. Cavalli[24b,24a], L.J. Caviedes Betancourt[23b], Y.C. Cekmecelioglu[49], E. Celebi[83], S. Cella[37], F. Celli[129], M.S. Centonze[71a,71b], V. Cepaitis[57], K. Cerny[125], A.S. Cerqueira[84a], A. Cerri[149],

JHEP10(2024)104

L. Cerrito[77a,77b], F. Cerutti[18a], B. Cervato[144], A. Cervelli[24b], G. Cesarini[54], S.A. Cetin[83], D. Chakraborty[118], J. Chan[18a], W.Y. Chan[156], J.D. Chapman[33], E. Chapon[138], B. Chargeishvili[152b], D.G. Charlton[21], M. Chatterjee[20], C. Chauhan[136], Y. Che[114a], S. Chekanov[6], S.V. Chekulaev[159a], G.A. Chelkov[39,a], A. Chen[108], B. Chen[154], B. Chen[168], H. Chen[114a], H. Chen[30], J. Chen[63c], J. Chen[145], M. Chen[129], S. Chen[156], S.J. Chen[114a], X. Chen[63c], X. Chen[15,ad], Y. Chen[63a], C.L. Cheng[173], H.C. Cheng[65a], S. Cheong[146], A. Cheplakov[39], E. Cheremushkina[49], E. Cherepanova[117], R. Cherkaoui El Moursli[36e], E. Cheu[7], K. Cheung[66], L. Chevalier[138], V. Chiarella[54], G. Chiarelli[75a], N. Chiedde[104], G. Chiodini[71a], A.S. Chisholm[21], A. Chitan[28b], M. Chitishvili[166], M.V. Chizhov[39,r], K. Choi[11], Y. Chou[141], E.Y.S. Chow[116], K.L. Chu[172], M.C. Chu[65a], X. Chu[14,114c], Z. Chubinidze[54], J. Chudoba[134], J.J. Chwastowski[88], D. Cieri[112], K.M. Ciesla[87a], V. Cindro[95], A. Ciocio[18a], F. Cirotto[73a,73b], Z.H. Citron[172], M. Citterio[72a], D.A. Ciubotaru[28b], A. Clark[57], P.J. Clark[53], N. Clarke Hall[98], C. Clarry[158], J.M. Clavijo Columbie[49], S.E. Clawson[49], C. Clement[48a,48b], Y. Coadou[104], M. Cobal[70a,70c], A. Coccaro[58b], R.F. Coelho Barrue[133a], R. Coelho Lopes De Sa[105], S. Coelli[72a], B. Cole[42], J. Collot[61], P. Conde Muiño[133a,133g], M.P. Connell[34c], S.H. Connell[34c], E.I. Conroy[129], F. Conventi[73a,af], H.G. Cooke[21], A.M. Cooper-Sarkar[129], F.A. Corchia[24b,24a], A. Cordeiro Oudot Choi[130], L.D. Corpe[41], M. Corradi[76a,76b], F. Corriveau[106,x], A. Cortes-Gonzalez[19], M.J. Costa[166], F. Costanza[4], D. Costanzo[142], B.M. Cote[122], J. Couthures[4], G. Cowan[97], K. Cranmer[173], D. Cremonini[24b,24a], S. Crépé-Renaudin[61], F. Crescioli[130], M. Cristinziani[144], M. Cristoforetti[79a,79b], V. Croft[117], J.E. Crosby[124], G. Crosetti[44b,44a], A. Cueto[101], H. Cui[98], Z. Cui[7], W.R. Cunningham[60], F. Curcio[166], J.R. Curran[53], P. Czodrowski[37], M.J. Da Cunha Sargedas De Sousa[58b,58a], J.V. Da Fonseca Pinto[84b], C. Da Via[103], W. Dabrowski[87a], T. Dado[37], S. Dahbi[151], T. Dai[108], D. Dal Santo[20], C. Dallapiccola[105], M. Dam[43], G. D'amen[30], V. D'Amico[111], J. Damp[102], J.R. Dandoy[35], D. Dannheim[37], M. Danninger[145], V. Dao[148], G. Darbo[58b], S.J. Das[30,ag], F. Dattola[49], S. D'Auria[72a,72b], A. D'Avanzo[73a,73b], C. David[34a], T. Davidek[136], I. Dawson[96], H.A. Day-hall[135], K. De[8], R. De Asmundis[73a], N. De Biase[49], S. De Castro[24b,24a], N. De Groot[116], P. de Jong[117], H. De la Torre[118], A. De Maria[114a], A. De Salvo[76a], U. De Sanctis[77a,77b], F. De Santis[71a,71b], A. De Santo[149], J.B. De Vivie De Regie[61], D.V. Dedovich[39], J. Degens[94], A.M. Deiana[45], F. Del Corso[24b,24a], J. Del Peso[101], F. Del Rio[64a], L. Delagrange[130], F. Deliot[138], C.M. Delitzsch[50], M. Della Pietra[73a,73b], D. Della Volpe[57], A. Dell'Acqua[37], L. Dell'Asta[72a,72b], M. Delmastro[4], P.A. Delsart[61], S. Demers[175], M. Demichev[39], S.P. Denisov[38], L. D'Eramo[41], D. Derendarz[88], F. Derue[130], P. Dervan[94], K. Desch[25], C. Deutsch[25], F.A. Di Bello[58b,58a], A. Di Ciaccio[77a,77b], L. Di Ciaccio[4], A. Di Domenico[76a,76b], C. Di Donato[73a,73b], A. Di Girolamo[37], G. Di Gregorio[37], A. Di Luca[79a,79b], B. Di Micco[78a,78b], R. Di Nardo[78a,78b], K.F. Di Petrillo[40], M. Diamantopoulou[35], F.A. Dias[117], T. Dias Do Vale[145], M.A. Diaz[140a,140b], F.G. Diaz Capriles[25], A.R. Didenko[39], M. Didenko[166], E.B. Diehl[108], S. Díez Cornell[49], C. Diez Pardos[144], C. Dimitriadi[164], A. Dimitrievska[21], J. Dingfelder[25], T. Dingley[129], I-M. Dinu[28b], S.J. Dittmeier[64b], F. Dittus[37], M. Divisek[136], F. Djama[104], T. Djobava[152b], C. Doglioni[103,100], A. Dohnalova[29a], J. Dolejsi[136], Z. Dolezal[136],

K. Domijan[87a], K.M. Dona[40], M. Donadelli[84d], B. Dong[109], J. Donini[41],
A. D'Onofrio[73a,73b], M. D'Onofrio[94], J. Dopke[137], A. Doria[73a],
N. Dos Santos Fernandes[133a], P. Dougan[103], M.T. Dova[92], A.T. Doyle[60], M.A. Draguet[129],
E. Dreyer[172], I. Drivas-koulouris[10], M. Drnevich[120], M. Drozdova[57], D. Du[63a],
T.A. du Pree[117], F. Dubinin[38], M. Dubovsky[29a], E. Duchovni[172], G. Duckeck[111],
O.A. Ducu[28b], D. Duda[53], A. Dudarev[37], E.R. Duden[27], M. D'uffizi[103], L. Duflot[67],
M. Dührssen[37], I. Duminica[28g], A.E. Dumitriu[28b], M. Dunford[64a], S. Dungs[50],
K. Dunne[48a,48b], A. Duperrin[104], H. Duran Yildiz[3a], M. Düren[59], A. Durglishvili[152b],
B.L. Dwyer[118], G.I. Dyckes[18a], M. Dyndal[87a], B.S. Dziedzic[37], Z.O. Earnshaw[149],
G.H. Eberwein[129], B. Eckerova[29a], S. Eggebrecht[56], E. Egidio Purcino De Souza[84e],
L.F. Ehrke[57], G. Eigen[17], K. Einsweiler[18a], T. Ekelof[164], P.A. Ekman[100], S. El Farkh[36b],
Y. El Ghazali[63a], H. El Jarrari[37], A. El Moussaouy[36a], V. Ellajosyula[164], M. Ellert[164],
F. Ellinghaus[174], N. Ellis[37], J. Elmsheuser[30], M. Elsawy[119a], M. Elsing[37],
D. Emeliyanov[137], Y. Enari[85], I. Ene[18a], S. Epari[13], P.A. Erland[88],
D. Ernani Martins Neto[88], M. Errenst[174], M. Escalier[67], C. Escobar[166], E. Etzion[154],
G. Evans[133a], H. Evans[69], L.S. Evans[97], A. Ezhilov[38], S. Ezzarqtouni[36a],
F. Fabbri[24b,24a], L. Fabbri[24b,24a], G. Facini[98], V. Fadeyev[139], R.M. Fakhrutdinov[38],
D. Fakoudis[102], S. Falciano[76a], L.F. Falda Ulhoa Coelho[37], F. Fallavollita[112],
G. Falsetti[44b,44a], J. Faltova[136], C. Fan[165], Y. Fan[14], Y. Fang[14,114c], M. Fanti[72a,72b],
M. Faraj[70a,70b], Z. Farazpay[99], A. Farbin[8], A. Farilla[78a], T. Farooque[109],
S.M. Farrington[53], F. Fassi[36e], D. Fassouliotis[9], M. Faucci Giannelli[77a,77b], W.J. Fawcett[33],
L. Fayard[67], P. Federic[136], P. Federicova[134], O.L. Fedin[38,a], M. Feickert[173],
L. Feligioni[104], D.E. Fellers[126], C. Feng[63b], Z. Feng[117], M.J. Fenton[162], L. Ferencz[49],
R.A.M. Ferguson[93], S.I. Fernandez Luengo[140f], P. Fernandez Martinez[13], M.J.V. Fernoux[104],
J. Ferrando[93], A. Ferrari[164], P. Ferrari[117,116], R. Ferrari[74a], D. Ferrere[57], C. Ferretti[108],
D. Fiacco[76a,76b], F. Fiedler[102], P. Fiedler[135], A. Filipčič[95], E.K. Filmer[1], F. Filthaut[116],
M.C.N. Fiolhais[133a,133c,c], L. Fiorini[166], W.C. Fisher[109], T. Fitschen[103], P.M. Fitzhugh[138],
I. Fleck[144], P. Fleischmann[108], T. Flick[174], M. Flores[34d,ab], L.R. Flores Castillo[65a],
L. Flores Sanz De Acedo[37], F.M. Follega[79a,79b], N. Fomin[33], J.H. Foo[158], A. Formica[138],
A.C. Forti[103], E. Fortin[37], A.W. Fortman[18a], M.G. Foti[18a], L. Fountas[9,j], D. Fournier[67],
H. Fox[93], P. Francavilla[75a,75b], S. Francescato[62], S. Franchellucci[57], M. Franchini[24b,24a],
S. Franchino[64a], D. Francis[37], L. Franco[116], V. Franco Lima[37], L. Franconi[49],
M. Franklin[62], G. Frattari[27], Y.Y. Frid[154], J. Friend[60], N. Fritzsche[37], A. Froch[55],
D. Froidevaux[37], J.A. Frost[129], Y. Fu[63a], S. Fuenzalida Garrido[140f], M. Fujimoto[104],
K.Y. Fung[65a], E. Furtado De Simas Filho[84e], M. Furukawa[156], J. Fuster[166], A. Gaa[56],
A. Gabrielli[24b,24a], A. Gabrielli[158], P. Gadow[37], G. Gagliardi[58b,58a], L.G. Gagnon[18a],
S. Gaid[163], S. Galantzan[154], E.J. Gallas[129], B.J. Gallop[137], K.K. Gan[122], S. Ganguly[156],
Y. Gao[53], F.M. Garay Walls[140a,140b], B. Garcia[30], C. García[166], A. Garcia Alonso[117],
A.G. Garcia Caffaro[175], J.E. García Navarro[166], M. Garcia-Sciveres[18a], G.L. Gardner[131],
R.W. Gardner[40], N. Garelli[161], D. Garg[81], R.B. Garg[146], J.M. Gargan[53], C.A. Garner[158],
C.M. Garvey[34a], V.K. Gassmann[161], G. Gaudio[74a], V. Gautam[13], P. Gauzzi[76a,76b],
J. Gavranovic[95], I.L. Gavrilenko[38], A. Gavrilyuk[38], C. Gay[167], G. Gaycken[126],
E.N. Gazis[10], A.A. Geanta[28b], C.M. Gee[139], A. Gekow[122], C. Gemme[58b], M.H. Genest[61],

A.D. Gentry[115], S. George[97], W.F. George[21], T. Geralis[47], P. Gessinger-Befurt[37], M.E. Geyik[174], M. Ghani[170], K. Ghorbanian[96], A. Ghosal[144], A. Ghosh[162], A. Ghosh[7], B. Giacobbe[24b], S. Giagu[76a,76b], T. Giani[117], A. Giannini[63a], S.M. Gibson[97], M. Gignac[139], D.T. Gil[87b], A.K. Gilbert[87a], B.J. Gilbert[42], D. Gillberg[35], G. Gilles[117], L. Ginabat[130], D.M. Gingrich[2,ae], M.P. Giordani[70a,70c], P.F. Giraud[138], G. Giugliarelli[70a,70c], D. Giugni[72a], F. Giuli[37], I. Gkialas[9,j], L.K. Gladilin[38], C. Glasman[101], G.R. Gledhill[126], G. Glemža[49], M. Glisic[126], I. Gnesi[44b,e], Y. Go[30], M. Goblirsch-Kolb[37], B. Gocke[50], D. Godin[110], B. Gokturk[22a], S. Goldfarb[107], T. Golling[57], M.G.D. Gololo[34g], D. Golubkov[38], J.P. Gombas[109], A. Gomes[133a,133b], G. Gomes Da Silva[144], A.J. Gomez Delegido[166], R. Gonçalo[133a], L. Gonella[21], A. Gongadze[152c], F. Gonnella[21], J.L. Gonski[146], R.Y. González Andana[53], S. González de la Hoz[166], R. Gonzalez Lopez[94], C. Gonzalez Renteria[18a], M.V. Gonzalez Rodrigues[49], R. Gonzalez Suarez[164], S. Gonzalez-Sevilla[57], L. Goossens[37], B. Gorini[37], E. Gorini[71a,71b], A. Gorišek[95], T.C. Gosart[131], A.T. Goshaw[52], M.I. Gostkin[39], S. Goswami[124], C.A. Gottardo[37], S.A. Gotz[111], M. Gouighri[36b], V. Goumarre[49], A.G. Goussiou[141], N. Govender[34c], R.P. Grabarczyk[129], I. Grabowska-Bold[87a], K. Graham[35], E. Gramstad[128], S. Grancagnolo[71a,71b], C.M. Grant[1,138], P.M. Gravila[28f], F.G. Gravili[71a,71b], H.M. Gray[18a], M. Greco[71a,71b], M.J. Green[1], C. Grefe[25], A.S. Grefsrud[17], I.M. Gregor[49], K.T. Greif[162], P. Grenier[146], S.G. Grewe[112], A.A. Grillo[139], K. Grimm[32], S. Grinstein[13,t], J.-F. Grivaz[67], E. Gross[172], J. Grosse-Knetter[56], J.C. Grundy[129], L. Guan[108], J.G.R. Guerrero Rojas[166], G. Guerrieri[37], R. Gugel[102], J.A.M. Guhit[108], A. Guida[19], E. Guilloton[170], S. Guindon[37], F. Guo[14,114c], J. Guo[63c], L. Guo[49], Y. Guo[108], R. Gupta[132], S. Gurbuz[25], S.S. Gurdasani[55], G. Gustavino[76a,76b], P. Gutierrez[123], L.F. Gutierrez Zagazeta[131], M. Gutsche[51], C. Gutschow[98], C. Gwenlan[129], C.B. Gwilliam[94], E.S. Haaland[128], A. Haas[120], M. Habedank[49], C. Haber[18a], H.K. Hadavand[8], A. Hadef[51], S. Hadzic[112], A.I. Hagan[93], J.J. Hahn[144], E.H. Haines[98], M. Haleem[169], J. Haley[124], J.J. Hall[142], G.D. Hallewell[104], L. Halser[20], K. Hamano[168], M. Hamer[25], G.N. Hamity[53], E.J. Hampshire[97], J. Han[63b], K. Han[63a], L. Han[114a], L. Han[63a], S. Han[18a], Y.F. Han[158], K. Hanagaki[85], M. Hance[139], D.A. Hangal[42], H. Hanif[145], M.D. Hank[131], J.B. Hansen[43], P.H. Hansen[43], D. Harada[57], T. Harenberg[174], S. Harkusha[38], M.L. Harris[105], Y.T. Harris[129], J. Harrison[13], N.M. Harrison[122], P.F. Harrison[170], N.M. Hartman[112], N.M. Hartmann[111], R.Z. Hasan[97,137], Y. Hasegawa[143], F. Haslbeck[129], S. Hassan[17], R. Hauser[109], C.M. Hawkes[21], R.J. Hawkings[37], Y. Hayashi[156], D. Hayden[109], C. Hayes[108], R.L. Hayes[117], C.P. Hays[129], J.M. Hays[96], H.S. Hayward[94], F. He[63a], M. He[14,114c], Y. He[49], Y. He[98], N.B. Heatley[96], V. Hedberg[100], A.L. Heggelund[128], N.D. Hehir[96,*], C. Heidegger[55], K.K. Heidegger[55], J. Heilman[35], S. Heim[49], T. Heim[18a], J.G. Heinlein[131], J.J. Heinrich[126], L. Heinrich[112,ac], J. Hejbal[134], A. Held[173], S. Hellesund[17], C.M. Helling[167], S. Hellman[48a,48b], R.C.W. Henderson[93], L. Henkelmann[33], A.M. Henriques Correia[37], H. Herde[100], Y. Hernández Jiménez[148], L.M. Herrmann[25], T. Herrmann[51], G. Herten[55], R. Hertenberger[111], L. Hervas[37], M.E. Hesping[102], N.P. Hessey[159a], M. Hidaoui[36b], N. Hidic[136], E. Hill[158], S.J. Hillier[21], J.R. Hinds[109], F. Hinterkeuser[25], M. Hirose[127], S. Hirose[160], D. Hirschbuehl[174], T.G. Hitchings[103], B. Hiti[95], J. Hobbs[148], R. Hobincu[28e], N. Hod[172], M.C. Hodgkinson[142], B.H. Hodkinson[129], A. Hoecker[37], D.D. Hofer[108], J. Hofer[49], T. Holm[25], M. Holzbock[37], L.B.A.H. Hommels[33], B.P. Honan[103], J.J. Hong[69], J. Hong[63c], T.M. Hong[132], B.H. Hooberman[165], W.H. Hopkins[6], M.C. Hoppesch[165], Y. Horii[113], S. Hou[151], A.S. Howard[95], J. Howarth[60], J. Hoya[6], M. Hrabovsky[125], A. Hrynevich[49], T. Hryn'ova[4], P.J. Hsu[66], S.-C. Hsu[141], T. Hsu[67], M. Hu[18a], Q. Hu[63a], S. Huang[65b], X. Huang[14,114c], Y. Huang[142], Y. Huang[102], Y. Huang[14], Z. Huang[103], Z. Hubacek[135], M. Huebner[25], F. Huegging[25], T.B. Huffman[129], C.A. Hugli[49], M. Huhtinen[37], S.K. Huiberts[17], R. Hulsken[106], N. Huseynov[12,g], J. Huston[109], J. Huth[62], R. Hyneman[146], G. Iacobucci[57], G. Iakovidis[30], L. Iconomidou-Fayard[67], J.P. Iddon[37], P. Iengo[73a,73b], R. Iguchi[156], Y. Iiyama[156], T. Iizawa[129], Y. Ikegami[85], N. Ilic[158], H. Imam[84c], M. Ince Lezki[57], T. Ingebretsen Carlson[48a,48b], J.M. Inglis[96], G. Introzzi[74a,74b], M. Iodice[78a], V. Ippolito[76a,76b], R.K. Irwin[94], M. Ishino[156], W. Islam[173], C. Issever[19,49], S. Istin[22a,ai], H. Ito[171], R. Iuppa[79a,79b], A. Ivina[172], J.M. Izen[46], V. Izzo[73a], P. Jacka[134], P. Jackson[1], C.S. Jagfeld[111], G. Jain[159a], P. Jain[49], K. Jakobs[55], T. Jakoubek[172], J. Jamieson[60], W. Jang[156], M. Javurkova[105], P. Jawahar[103], L. Jeanty[126], J. Jejelava[152a,aa], P. Jenni[55,f], C.E. Jessiman[35], C. Jia[63b], J. Jia[148], X. Jia[62], X. Jia[14,114c], Z. Jia[114a], C. Jiang[53], S. Jiggins[49], J. Jimenez Pena[13], S. Jin[114a], A. Jinaru[28b], O. Jinnouchi[157], P. Johansson[142], K.A. Johns[7], J.W. Johnson[139], F.A. Jolly[49], D.M. Jones[149], E. Jones[49], K.S. Jones[8], P. Jones[33], R.W.L. Jones[93], T.J. Jones[94], H.L. Joos[56,37], R. Joshi[122], J. Jovicevic[16], X. Ju[18a], J.J. Junggeburth[105], T. Junkermann[64a], A. Juste Rozas[13,t], M.K. Juzek[88], S. Kabana[140e], A. Kaczmarska[88], M. Kado[112], H. Kagan[122], M. Kagan[146], A. Kahn[131], C. Kahra[102], T. Kaji[156], E. Kajomovitz[153], N. Kakati[172], I. Kalaitzidou[55], C.W. Kalderon[30], N.J. Kang[139], D. Kar[34g], K. Karava[129], M.J. Kareem[159b], E. Karentzos[55], O. Karkout[117], S.N. Karpov[39], Z.M. Karpova[39], V. Kartvelishvili[93], A.N. Karyukhin[38], E. Kasimi[155], J. Katzy[49], S. Kaur[35], K. Kawade[143], M.P. Kawale[123], C. Kawamoto[89], T. Kawamoto[63a], E.F. Kay[37], F.I. Kaya[161], S. Kazakos[109], V.F. Kazanin[38], Y. Ke[148], J.M. Keaveney[34a], R. Keeler[168], G.V. Kehris[62], J.S. Keller[35], A.S. Kelly[98], J.J. Kempster[149], P.D. Kennedy[102], O. Kepka[134], B.P. Kerridge[137], S. Kersten[174], B.P. Kerševan[95], L. Keszeghova[29a], S. Ketabchi Haghighat[158], R.A. Khan[132], A. Khanov[124], A.G. Kharlamov[38], T. Kharlamova[38], E.E. Khoda[141], M. Kholodenko[133a], T.J. Khoo[19], G. Khoriauli[169], J. Khubua[152b,*], Y.A.R. Khwaira[130], B. Kibirige[34g], D. Kim[6], D.W. Kim[48a,48b], Y.K. Kim[40], N. Kimura[98], M.K. Kingston[56], A. Kirchhoff[56], C. Kirfel[25], F. Kirfel[25], J. Kirk[137], A.E. Kiryunin[112], C. Kitsaki[10], O. Kivernyk[25], M. Klassen[161], C. Klein[35], L. Klein[169], M.H. Klein[45], S.B. Klein[57], U. Klein[94], P. Klimek[37], A. Klimentov[30], T. Klioutchnikova[37], P. Kluit[117], S. Kluth[112], E. Kneringer[80], T.M. Knight[158], A. Knue[50], D. Kobylianskii[172], S.F. Koch[129], M. Kocian[146], P. Kodyš[136], D.M. Koeck[126], P.T. Koenig[25], T. Koffas[35], O. Kolay[51], I. Koletsou[4], T. Komarek[88], K. Köneke[55], A.X.Y. Kong[1], T. Kono[121], N. Konstantinidis[98], P. Kontaxakis[57], B. Konya[100], R. Kopeliansky[42], S. Koperny[87a], K. Korcyl[88], K. Kordas[155,d], A. Korn[98], S. Korn[56], I. Korolkov[13], N. Korotkova[38], B. Kortman[117], O. Kortner[112], S. Kortner[112], W.H. Kostecka[118], V.V. Kostyukhin[144],

A. Kotsokechagia[37], A. Kotwal[52], A. Koulouris[37], A. Kourkoumeli-Charalampidi[74a,74b], C. Kourkoumelis[9], E. Kourlitis[112,ac], O. Kovanda[126], R. Kowalewski[168], W. Kozanecki[138], A.S. Kozhin[38], V.A. Kramarenko[38], G. Kramberger[95], P. Kramer[102], M.W. Krasny[130], A. Krasznahorkay[37], A.C. Kraus[118], J.W. Kraus[174], J.A. Kremer[49], T. Kresse[51], L. Kretschmann[174], J. Kretzschmar[94], K. Kreul[19], P. Krieger[158], M. Krivos[136], K. Krizka[21], K. Kroeninger[50], H. Kroha[112], J. Kroll[134], J. Kroll[131], K.S. Krowpman[109], U. Kruchonak[39], H. Krüger[25], N. Krumnack[82], M.C. Kruse[52], O. Kuchinskaia[38], S. Kuday[3a], S. Kuehn[37], R. Kuesters[55], T. Kuhl[49], V. Kukhtin[39], Y. Kulchitsky[38,a], S. Kuleshov[140d,140b], M. Kumar[34g], N. Kumari[49], P. Kumari[159b], A. Kupco[134], T. Kupfer[50], A. Kupich[38], O. Kuprash[55], H. Kurashige[86], L.L. Kurchaninov[159a], O. Kurdysh[67], Y.A. Kurochkin[38], A. Kurova[38], M. Kuze[157], A.K. Kvam[105], J. Kvita[125], T. Kwan[106], N.G. Kyriacou[108], L.A.O. Laatu[104], C. Lacasta[166], F. Lacava[76a,76b], H. Lacker[19], D. Lacour[130], N.N. Lad[98], E. Ladygin[39], A. Lafarge[41], B. Laforge[130], T. Lagouri[175], F.Z. Lahbabi[36a], S. Lai[56], J.E. Lambert[168], S. Lammers[69], W. Lampl[7], C. Lampoudis[155,d], G. Lamprinoudis[102], A.N. Lancaster[118], E. Lançon[30], U. Landgraf[55], M.P.J. Landon[96], V.S. Lang[55], O.K.B. Langrekken[128], A.J. Lankford[162], F. Lanni[37], K. Lantzsch[25], A. Lanza[74a], J.F. Laporte[138], T. Lari[72a], F. Lasagni Manghi[24b], M. Lassnig[37], V. Latonova[134], A. Laurier[153], S.D. Lawlor[142], Z. Lawrence[103], R. Lazaridou[170], M. Lazzaroni[72a,72b], B. Le[103], E.M. Le Boulicaut[52], L.T. Le Pottier[18a], B. Leban[24b,24a], A. Lebedev[82], M. LeBlanc[103], F. Ledroit-Guillon[61], S.C. Lee[151], S. Lee[48a,48b], T.F. Lee[94], L.L. Leeuw[34c], H.P. Lefebvre[97], M. Lefebvre[168], C. Leggett[18a], G. Lehmann Miotto[37], M. Leigh[57], W.A. Leight[105], W. Leinonen[116], A. Leisos[155,s], M.A.L. Leite[84c], C.E. Leitgeb[19], R. Leitner[136], K.J.C. Leney[45], T. Lenz[25], S. Leone[75a], C. Leonidopoulos[53], A. Leopold[147], R. Les[109], C.G. Lester[33], M. Levchenko[38], J. Levêque[4], L.J. Levinson[172], G. Levrini[24b,24a], M.P. Lewicki[88], C. Lewis[141], D.J. Lewis[4], A. Li[5], B. Li[63b], C. Li[63a], C-Q. Li[112], H. Li[63a], H. Li[63b], H. Li[114a], H. Li[15], H. Li[63b], J. Li[63c], K. Li[141], L. Li[63c], M. Li[14,114c], S. Li[14,114c], S. Li[63d,63c], T. Li[5], X. Li[106], Z. Li[129], Z. Li[156], Z. Li[14,114c], Z. Li[63a], S. Liang[14,114c], Z. Liang[14], M. Liberatore[138], B. Liberti[77a], K. Lie[65c], J. Lieber Marin[84e], H. Lien[69], H. Lin[108], K. Lin[109], R.E. Lindley[7], J.H. Lindon[2], J. Ling[62], E. Lipeles[131], A. Lipniacka[17], A. Lister[167], J.D. Little[69], B. Liu[14], B.X. Liu[114b], D. Liu[63d,63c], E.H.L. Liu[21], J.B. Liu[63a], J.K.K. Liu[33], K. Liu[63d], K. Liu[63d,63c], M. Liu[63a], M.Y. Liu[63a], P. Liu[14], Q. Liu[63d,141,63c], X. Liu[63a], X. Liu[63b], Y. Liu[114b,114c], Y.L. Liu[63b], Y.W. Liu[63a], S.L. Lloyd[96], E.M. Lobodzinska[49], P. Loch[7], T. Lohse[19], K. Lohwasser[142], E. Loiacono[49], M. Lokajicek[134,*], J.D. Lomas[21], J.D. Long[165], I. Longarini[162], R. Longo[165], I. Lopez Paz[68], A. Lopez Solis[49], N.A. Lopez-canelas[7], N. Lorenzo Martinez[4], A.M. Lory[111], M. Losada[119a], G. Löschcke Centeno[149], O. Loseva[38], X. Lou[48a,48b], X. Lou[14,114c], A. Lounis[67], P.A. Love[93], G. Lu[14,114c], M. Lu[67], S. Lu[131], Y.J. Lu[66], H.J. Lubatti[141], C. Luci[76a,76b], F.L. Lucio Alves[114a], F. Luehring[69], I. Luise[148], O. Lukianchuk[67], O. Lundberg[147], B. Lund-Jensen[147,*], N.A. Luongo[6], M.S. Lutz[37], A.B. Lux[26], D. Lynn[30], R. Lysak[134], E. Lytken[100], V. Lyubushkin[39], T. Lyubushkina[39], M.M. Lyukova[148], M.Firdaus M. Soberi[53], H. Ma[30], K. Ma[63a], L.L. Ma[63b], W. Ma[63a], Y. Ma[124], J.C. MacDonald[102], P.C. Machado De Abreu Farias[84e], R. Madar[41],

T. Madula[98], J. Maeda[86], T. Maeno[30], H. Maguire[142], V. Maiboroda[138], A. Maio[133a,133b,133d], K. Maj[87a], O. Majersky[49], S. Majewski[126], N. Makovec[67], V. Maksimovic[16], B. Malaescu[130], Pa. Malecki[88], V.P. Maleev[38], F. Malek[61,n], M. Mali[95], D. Malito[97], U. Mallik[81,*], S. Maltezos[10], S. Malyukov[39], J. Mamuzic[13], G. Mancini[54], M.N. Mancini[27], G. Manco[74a,74b], J.P. Mandalia[96], S.S. Mandarry[149], I. Mandić[95], L. Manhaes de Andrade Filho[84a], I.M. Maniatis[172], J. Manjarres Ramos[91], D.C. Mankad[172], A. Mann[111], S. Manzoni[37], L. Mao[63c], X. Mapekula[34c], A. Marantis[155,s], G. Marchiori[5], M. Marcisovsky[134], C. Marcon[72a], M. Marinescu[21], S. Marium[49], M. Marjanovic[123], A. Markhoos[55], M. Markovitch[67], E.J. Marshall[93], Z. Marshall[18a], S. Marti-Garcia[166], J. Martin[98], T.A. Martin[137], V.J. Martin[53], B. Martin dit Latour[17], L. Martinelli[76a,76b], M. Martinez[13,t], P. Martinez Agullo[166], V.I. Martinez Outschoorn[105], P. Martinez Suarez[13], S. Martin-Haugh[137], G. Martinovicova[136], V.S. Martoiu[28b], A.C. Martyniuk[98], A. Marzin[37], D. Mascione[79a,79b], L. Masetti[102], J. Masik[103], A.L. Maslennikov[38], P. Massarotti[73a,73b], P. Mastrandrea[75a,75b], A. Mastroberardino[44b,44a], T. Masubuchi[127], T. Mathisen[164], J. Matousek[136], J. Maurer[28b], A.J. Maury[67], B. Maček[95], D.A. Maximov[38], A.E. May[103], R. Mazini[151], I. Maznas[118], M. Mazza[109], S.M. Mazza[139], E. Mazzeo[72a,72b], C. Mc Ginn[30], J.P. Mc Gowan[168], S.P. Mc Kee[108], C.C. McCracken[167], E.F. McDonald[107], A.E. McDougall[117], J.A. Mcfayden[149], R.P. McGovern[131], R.P. Mckenzie[34g], T.C. Mclachlan[49], D.J. Mclaughlin[98], S.J. McMahon[137], C.M. Mcpartland[94], R.A. McPherson[168,x], S. Mehlhase[111], A. Mehta[94], D. Melini[166], B.R. Mellado Garcia[34g], A.H. Melo[56], F. Meloni[49], A.M. Mendes Jacques Da Costa[103], H.Y. Meng[158], L. Meng[93], S. Menke[112], M. Mentink[37], E. Meoni[44b,44a], G. Mercado[118], S. Merianos[155], C. Merlassino[70a,70c], L. Merola[73a,73b], C. Meroni[72a,72b], J. Metcalfe[6], A.S. Mete[6], E. Meuser[102], C. Meyer[69], J-P. Meyer[138], R.P. Middleton[137], L. Mijović[53], G. Mikenberg[172], M. Mikestikova[134], M. Mikuž[95], H. Mildner[102], A. Milic[37], D.W. Miller[40], E.H. Miller[146], L.S. Miller[35], A. Milov[172], D.A. Milstead[48a,48b], T. Min[114a], A.A. Minaenko[38], I.A. Minashvili[152b], L. Mince[60], A.I. Mincer[120], B. Mindur[87a], M. Mineev[39], Y. Mino[89], L.M. Mir[13], M. Miralles Lopez[60], M. Mironova[18a], M.C. Missio[116], A. Mitra[170], V.A. Mitsou[166], Y. Mitsumori[113], O. Miu[158], P.S. Miyagawa[96], T. Mkrtchyan[64a], M. Mlinarevic[98], T. Mlinarevic[98], M. Mlynarikova[37], S. Mobius[20], P. Mogg[111], M.H. Mohamed Farook[115], A.F. Mohammed[14,114c], S. Mohapatra[42], G. Mokgatitswane[34g], L. Moleri[172], B. Mondal[144], S. Mondal[135], K. Mönig[49], E. Monnier[104], L. Monsonis Romero[166], J. Montejo Berlingen[13], A. Montella[48a,48b], M. Montella[122], F. Montereali[78a,78b], F. Monticelli[92], S. Monzani[70a,70c], A. Morancho Tarda[43], N. Morange[67], A.L. Moreira De Carvalho[49], M. Moreno Llácer[166], C. Moreno Martinez[57], P. Morettini[58b], S. Morgenstern[37], M. Morii[62], M. Morinaga[156], F. Morodei[76a,76b], L. Morvaj[37], P. Moschovakos[37], B. Moser[129], M. Mosidze[152b], T. Moskalets[45], P. Moskvitina[116], J. Moss[32,k], P. Moszkowicz[87a], A. Moussa[36d], E.J.W. Moyse[105], O. Mtintsilana[34g], S. Muanza[104], J. Mueller[132], D. Muenstermann[93], R. Müller[37], G.A. Mullier[164], A.J. Mullin[33], J.J. Mullin[131], D.P. Mungo[158], D. Munoz Perez[166], F.J. Munoz Sanchez[103], M. Murin[103], W.J. Murray[170,137], M. Muškinja[95], C. Mwewa[30], A.G. Myagkov[38,a], A.J. Myers[8], G. Myers[108], M. Myska[135], B.P. Nachman[18a], O. Nackenhorst[50],

K. Nagai[129], K. Nagano[85], J.L. Nagle[30,ag], E. Nagy[104], A.M. Nairz[37], Y. Nakahama[85], K. Nakamura[85], K. Nakkalil[5], H. Nanjo[127], E.A. Narayanan[115], I. Naryshkin[38], L. Nasella[72a,72b], M. Naseri[35], S. Nasri[119b], C. Nass[25], G. Navarro[23a], J. Navarro-Gonzalez[166], R. Nayak[154], A. Nayaz[19], P.Y. Nechaeva[38], S. Nechaeva[24b,24a], F. Nechansky[49], L. Nedic[129], T.J. Neep[21], A. Negri[74a,74b], M. Negrini[24b], C. Nellist[117], C. Nelson[106], K. Nelson[108], S. Nemecek[134], M. Nessi[37,h], M.S. Neubauer[165], F. Neuhaus[102], J. Neundorf[49], P.R. Newman[21], C.W. Ng[132], Y.W.Y. Ng[49], B. Ngair[119a], H.D.N. Nguyen[110], R.B. Nickerson[129], R. Nicolaidou[138], J. Nielsen[139], M. Niemeyer[56], J. Niermann[56], N. Nikiforou[37], V. Nikolaenko[38,a], I. Nikolic-Audit[130], K. Nikolopoulos[21], P. Nilsson[30], I. Ninca[49], G. Ninio[154], A. Nisati[76a], N. Nishu[2], R. Nisius[112], J-E. Nitschke[51], E.K. Nkadimeng[34g], T. Nobe[156], T. Nommensen[150], M.B. Norfolk[142], B.J. Norman[35], M. Noury[36a], J. Novak[95], T. Novak[95], L. Novotny[135], R. Novotny[115], L. Nozka[125], K. Ntekas[162], N.M.J. Nunes De Moura Junior[84b], J. Ocariz[130], A. Ochi[86], I. Ochoa[133a], S. Oerdek[49,u], J.T. Offermann[40], A. Ogrodnik[136], A. Oh[103], C.C. Ohm[147], H. Oide[85], R. Oishi[156], M.L. Ojeda[49], Y. Okumura[156], L.F. Oleiro Seabra[133a], I. Oleksiyuk[57], S.A. Olivares Pino[140d], G. Oliveira Correa[13], D. Oliveira Damazio[30], J.L. Oliver[162], Ö.O. Öncel[55], A.P. O'Neill[20], A. Onofre[133a,133e], P.U.E. Onyisi[11], M.J. Oreglia[40], G.E. Orellana[92], D. Orestano[78a,78b], N. Orlando[13], R.S. Orr[158], L.M. Osojnak[131], R. Ospanov[63a], G. Otero y Garzon[31], H. Otono[90], P.S. Ott[64a], G.J. Ottino[18a], M. Ouchrif[36d], F. Ould-Saada[128], T. Ovsiannikova[141], M. Owen[60], R.E. Owen[137], V.E. Ozcan[22a], F. Ozturk[88], N. Ozturk[8], S. Ozturk[83], H.A. Pacey[129], A. Pacheco Pages[13], C. Padilla Aranda[13], G. Padovano[76a,76b], S. Pagan Griso[18a], G. Palacino[69], A. Palazzo[71a,71b], J. Pampel[25], J. Pan[175], T. Pan[65a], D.K. Panchal[11], C.E. Pandini[117], J.G. Panduro Vazquez[137], H.D. Pandya[1], H. Pang[15], P. Pani[49], G. Panizzo[70a,70c], L. Panwar[130], L. Paolozzi[57], S. Parajuli[165], A. Paramonov[6], C. Paraskevopoulos[54], D. Paredes Hernandez[65b], A. Pareti[74a,74b], K.R. Park[42], T.H. Park[158], M.A. Parker[33], F. Parodi[58b,58a], E.W. Parrish[118], V.A. Parrish[53], J.A. Parsons[42], U. Parzefall[55], B. Pascual Dias[110], L. Pascual Dominguez[101], E. Pasqualucci[76a], S. Passaggio[58b], F. Pastore[97], P. Patel[88], U.M. Patel[52], J.R. Pater[103], T. Pauly[37], C.I. Pazos[161], J. Pearkes[146], M. Pedersen[128], R. Pedro[133a], S.V. Peleganchuk[38], O. Penc[37], E.A. Pender[53], S. Peng[15], G.D. Penn[175], K.E. Penski[111], M. Penzin[38], B.S. Peralva[84d], A.P. Pereira Peixoto[141], L. Pereira Sanchez[146], D.V. Perepelitsa[30,ag], G. Perera[105], E. Perez Codina[159a], M. Perganti[10], H. Pernegger[37], S. Perrella[76a,76b], O. Perrin[41], K. Peters[49], R.F.Y. Peters[103], B.A. Petersen[37], T.C. Petersen[43], E. Petit[104], V. Petousis[135], C. Petridou[155,d], T. Petru[136], A. Petrukhin[144], M. Pettee[18a], A. Petukhov[38], K. Petukhova[37], R. Pezoa[140f], L. Pezzotti[37], G. Pezzullo[175], T.M. Pham[173], T. Pham[107], P.W. Phillips[137], G. Piacquadio[148], E. Pianori[18a], F. Piazza[126], R. Piegaia[31], D. Pietreanu[28b], A.D. Pilkington[103], M. Pinamonti[70a,70c], J.L. Pinfold[2], B.C. Pinheiro Pereira[133a], A.E. Pinto Pinoargote[138,138], L. Pintucci[70a,70c], K.M. Piper[149], A. Pirttikoski[57], D.A. Pizzi[35], L. Pizzimento[65b], A. Pizzini[117], M.-A. Pleier[30], V. Pleskot[136], E. Plotnikova[39], G. Poddar[96], R. Poettgen[100], L. Poggioli[130], I. Pokharel[56], S. Polacek[136], G. Polesello[74a], A. Poley[145,159a], A. Polini[24b], C.S. Pollard[170], Z.B. Pollock[122],

JHEP10(2024)104

E. Pompa Pacchi[76a,76b], N.I. Pond[98], D. Ponomarenko[116], L. Pontecorvo[37], S. Popa[28a], G.A. Popeneciu[28d], A. Poreba[37], D.M. Portillo Quintero[159a], S. Pospisil[135], M.A. Postill[142], P. Postolache[28c], K. Potamianos[170], P.A. Potepa[87a], I.N. Potrap[39], C.J. Potter[33], H. Potti[150], J. Poveda[166], M.E. Pozo Astigarraga[37], A. Prades Ibanez[77a,77b], J. Pretel[168], D. Price[103], M. Primavera[71a], L. Primomo[70a,70c], M.A. Principe Martin[101], R. Privara[125], T. Procter[60], M.L. Proffitt[141], N. Proklova[131], K. Prokofiev[65c], G. Proto[112], J. Proudfoot[6], M. Przybycien[87a], W.W. Przygoda[87b], A. Psallidas[47], J.E. Puddefoot[142], D. Pudzha[55], D. Pyatiizbyantseva[38], J. Qian[108], D. Qichen[103], Y. Qin[13], T. Qiu[53], A. Quadt[56], M. Queitsch-Maitland[103], G. Quetant[57], R.P. Quinn[167], G. Rabanal Bolanos[62], D. Rafanoharana[55], F. Raffaeli[77a,77b], F. Ragusa[72a,72b], J.L. Rainbolt[40], J.A. Raine[57], S. Rajagopalan[30], E. Ramakoti[38], L. Rambelli[58b,58a], I.A. Ramirez-Berend[35], K. Ran[49,114c], D.S. Rankin[131], N.P. Rapheeha[34g], H. Rasheed[28b], V. Raskina[130], D.F. Rassloff[64a], A. Rastogi[18a], S. Rave[102], S. Ravera[58b,58a], B. Ravina[56], I. Ravinovich[172], M. Raymond[37], A.L. Read[128], N.P. Readioff[142], D.M. Rebuzzi[74a,74b], G. Redlinger[30], A.S. Reed[112], K. Reeves[27], J.A. Reidelsturz[174], D. Reikher[126], A. Rej[50], C. Rembser[37], M. Renda[28b], F. Renner[49], A.G. Rennie[162], A.L. Rescia[49], S. Resconi[72a], M. Ressegotti[58b,58a], S. Rettie[37], J.G. Reyes Rivera[109], E. Reynolds[18a], O.L. Rezanova[38], P. Reznicek[136], H. Riani[36d], N. Ribaric[93], E. Ricci[79a,79b], R. Richter[112], S. Richter[48a,48b], E. Richter-Was[87b], M. Ridel[130], S. Ridouani[36d], P. Rieck[120], P. Riedler[37], E.M. Riefel[48a,48b], J.O. Rieger[117], M. Rijssenbeek[148], M. Rimoldi[37], L. Rinaldi[24b,24a], P. Rincke[56,164], T.T. Rinn[30], M.P. Rinnagel[111], G. Ripellino[164], I. Riu[13], J.C. Rivera Vergara[168], F. Rizatdinova[124], E. Rizvi[96], B.R. Roberts[18a], S.S. Roberts[139], S.H. Robertson[106,x], D. Robinson[33], M. Robles Manzano[102], A. Robson[60], A. Rocchi[77a,77b], C. Roda[75a,75b], S. Rodriguez Bosca[37], Y. Rodriguez Garcia[23a], A. Rodriguez Rodriguez[55], A.M. Rodríguez Vera[118], S. Roe[37], J.T. Roemer[37], A.R. Roepe-Gier[139], O. Røhne[128], R.A. Rojas[105], C.P.A. Roland[130], J. Roloff[30], A. Romaniouk[38], E. Romano[74a,74b], M. Romano[24b], A.C. Romero Hernandez[165], N. Rompotis[94], L. Roos[130], S. Rosati[76a], B.J. Rosser[40], E. Rossi[129], E. Rossi[73a,73b], L.P. Rossi[62], L. Rossini[55], R. Rosten[122], M. Rotaru[28b], B. Rottler[55], C. Rougier[91], D. Rousseau[67], D. Rousso[49], A. Roy[165], S. Roy-Garand[158], A. Rozanov[104], Z.M.A. Rozario[60], Y. Rozen[153], A. Rubio Jimenez[166], A.J. Ruby[94], V.H. Ruelas Rivera[19], T.A. Ruggeri[1], A. Ruggiero[129], A. Ruiz-Martinez[166], A. Rummler[37], Z. Rurikova[55], N.A. Rusakovich[39], H.L. Russell[168], G. Russo[76a,76b], J.P. Rutherfoord[7], S. Rutherford Colmenares[33], M. Rybar[136], E.B. Rye[128], A. Ryzhov[45], J.A. Sabater Iglesias[57], H.F-W. Sadrozinski[139], F. Safai Tehrani[76a], B. Safarzadeh Samani[137], S. Saha[1], M. Sahinsoy[83], A. Saibel[166], M. Saimpert[138], M. Saito[156], T. Saito[156], A. Sala[72a,72b], D. Salamani[37], A. Salnikov[146], J. Salt[166], A. Salvador Salas[154], D. Salvatore[44b,44a], F. Salvatore[149], A. Salzburger[37], D. Sammel[55], E. Sampson[93], D. Sampsonidis[155,d], D. Sampsonidou[126], J. Sánchez[166], V. Sanchez Sebastian[166], H. Sandaker[128], C.O. Sander[49], J.A. Sandesara[105], M. Sandhoff[174], C. Sandoval[23b], L. Sanfilippo[64a], D.P.C. Sankey[137], T. Sano[89], A. Sansoni[54], L. Santi[37,76b], C. Santoni[41], H. Santos[133a,133b], A. Santra[172], E. Sanzani[24b,24a], K.A. Saoucha[163], J.G. Saraiva[133a,133d], J. Sardain[7], O. Sasaki[85], K. Sato[160], C. Sauer[64b], E. Sauvan[4], P. Savard[158,ae], R. Sawada[156], C. Sawyer[137],

JHEP10(2024)104

L. Sawyer[99], C. Sbarra[24b], A. Sbrizzi[24b,24a], T. Scanlon[98], J. Schaarschmidt[141], U. Schäfer[102], A.C. Schaffer[67,45], D. Schaile[111], R.D. Schamberger[148], C. Scharf[19], M.M. Schefer[20], V.A. Schegelsky[38], D. Scheirich[136], M. Schernau[162], C. Scheulen[56], C. Schiavi[58b,58a], M. Schioppa[44b,44a], B. Schlag[146,m], K.E. Schleicher[55], S. Schlenker[37], J. Schmeing[174], M.A. Schmidt[174], K. Schmieden[102], C. Schmitt[102], N. Schmitt[102], S. Schmitt[49], L. Schoeffel[138], A. Schoening[64b], P.G. Scholer[35], E. Schopf[129], M. Schott[25], J. Schovancova[37], S. Schramm[57], T. Schroer[57], H-C. Schultz-Coulon[64a], M. Schumacher[55], B.A. Schumm[139], Ph. Schune[138], A.J. Schuy[141], H.R. Schwartz[139], A. Schwartzman[146], T.A. Schwarz[108], Ph. Schwemling[138], R. Schwienhorst[109], F.G. Sciacca[20], A. Sciandra[30], G. Sciolla[27], F. Scuri[75a], C.D. Sebastiani[94], K. Sedlaczek[118], S.C. Seidel[115], A. Seiden[139], B.D. Seidlitz[42], C. Seitz[49], J.M. Seixas[84b], G. Sekhniaidze[73a], L. Selem[61], N. Semprini-Cesari[24b,24a], D. Sengupta[57], V. Senthilkumar[166], L. Serin[67], M. Sessa[77a,77b], H. Severini[123], F. Sforza[58b,58a], A. Sfyrla[57], Q. Sha[14], E. Shabalina[56], A.H. Shah[33], R. Shaheen[147], J.D. Shahinian[131], D. Shaked Renous[172], L.Y. Shan[14], M. Shapiro[18a], A. Sharma[37], A.S. Sharma[167], P. Sharma[81], P.B. Shatalov[38], K. Shaw[149], S.M. Shaw[103], Q. Shen[63c], D.J. Sheppard[145], P. Sherwood[98], L. Shi[98], X. Shi[14], S. Shimizu[85], C.O. Shimmin[175], J.D. Shinner[97], I.P.J. Shipsey[129], S. Shirabe[90], M. Shiyakova[39,v], M.J. Shochet[40], D.R. Shope[128], B. Shrestha[123], S. Shrestha[122,ah], M.J. Shroff[168], P. Sicho[134], A.M. Sickles[165], E. Sideras Haddad[34g], A.C. Sidley[117], A. Sidoti[24b], F. Siegert[51], Dj. Sijacki[16], F. Sili[92], J.M. Silva[53], I. Silva Ferreira[84b], M.V. Silva Oliveira[30], S.B. Silverstein[48a], S. Simion[67], R. Simoniello[37], E.L. Simpson[103], H. Simpson[149], L.R. Simpson[108], N.D. Simpson[100], S. Simsek[83], S. Sindhu[56], P. Sinervo[158], S. Singh[158], S. Sinha[49], S. Sinha[103], M. Sioli[24b,24a], I. Siral[37], E. Sitnikova[49], J. Sjölin[48a,48b], A. Skaf[56], E. Skorda[21], P. Skubic[123], M. Slawinska[88], V. Smakhtin[172], B.H. Smart[137], S.Yu. Smirnov[38], Y. Smirnov[38], L.N. Smirnova[38,a], O. Smirnova[100], A.C. Smith[42], D.R. Smith[162], E.A. Smith[40], H.A. Smith[129], J.L. Smith[103], R. Smith[146], M. Smizanska[93], K. Smolek[135], A.A. Snesarev[38], S.R. Snider[158], H.L. Snoek[117], S. Snyder[30], R. Sobie[168,x], A. Soffer[154], C.A. Solans Sanchez[37], E.Yu. Soldatov[38], U. Soldevila[166], A.A. Solodkov[38], S. Solomon[27], A. Soloshenko[39], K. Solovieva[55], O.V. Solovyanov[41], P. Sommer[51], A. Sonay[13], W.Y. Song[159b], A. Sopczak[135], A.L. Sopio[98], F. Sopkova[29b], J.D. Sorenson[115], I.R. Sotarriva Alvarez[157], V. Sothilingam[64a], O.J. Soto Sandoval[140c,140b], S. Sottocornola[69], R. Soualah[163], Z. Soumaimi[36e], D. South[49], N. Soybelman[172], S. Spagnolo[71a,71b], M. Spalla[112], D. Sperlich[55], G. Spigo[37], B. Spisso[73a,73b], D.P. Spiteri[60], M. Spousta[136], E.J. Staats[35], R. Stamen[64a], A. Stampekis[21], M. Standke[25], E. Stanecka[88], W. Stanek-Maslouska[49], M.V. Stange[51], B. Stanislaus[18a], M.M. Stanitzki[49], B. Stapf[49], E.A. Starchenko[38], G.H. Stark[139], J. Stark[91], P. Staroba[134], P. Starovoitov[64a], S. Stärz[106], R. Staszewski[88], G. Stavropoulos[47], A. Stefl[37], P. Steinberg[30], B. Stelzer[145,159a], H.J. Stelzer[132], O. Stelzer-Chilton[159a], H. Stenzel[59], T.J. Stevenson[149], G.A. Stewart[37], J.R. Stewart[124], M.C. Stockton[37], G. Stoicea[28b], M. Stolarski[133a], S. Stonjek[112], A. Straessner[51], J. Strandberg[147], S. Strandberg[48a,48b], M. Stratmann[174], M. Strauss[123], T. Strebler[104], P. Strizenec[29b], R. Ströhmer[169], D.M. Strom[126], R. Stroynowski[45], A. Strubig[48a,48b], S.A. Stucci[30], B. Stugu[17], J. Stupak[123], N.A. Styles[49], D. Su[146], S. Su[63a], W. Su[63d],

X. Su[63a], D. Suchy[29a], K. Sugizaki[156], V.V. Sulin[38], M.J. Sullivan[94], D.M.S. Sultan[129], L. Sultanaliyeva[38], S. Sultansoy[3b], T. Sumida[89], S. Sun[173], O. Sunneborn Gudnadottir[164], N. Sur[104], M.R. Sutton[149], H. Suzuki[160], M. Svatos[134], M. Swiatlowski[159a], T. Swirski[169], I. Sykora[29a], M. Sykora[136], T. Sykora[136], D. Ta[102], K. Tackmann[49,u], A. Taffard[162], R. Tafirout[159a], J.S. Tafoya Vargas[67], Y. Takubo[85], M. Talby[104], A.A. Talyshev[38], K.C. Tam[65b], N.M. Tamir[154], A. Tanaka[156], J. Tanaka[156], R. Tanaka[67], M. Tanasini[148], Z. Tao[167], S. Tapia Araya[140f], S. Tapprogge[102], A. Tarek Abouelfadl Mohamed[109], S. Tarem[153], K. Tariq[14], G. Tarna[28b], G.F. Tartarelli[72a], M.J. Tartarin[91], P. Tas[136], M. Tasevsky[134], E. Tassi[44b,44a], A.C. Tate[165], G. Tateno[156], Y. Tayalati[36e,w], G.N. Taylor[107], W. Taylor[159b], R. Teixeira De Lima[146], P. Teixeira-Dias[97], J.J. Teoh[158], K. Terashi[156], J. Terron[101], S. Terzo[13], M. Testa[54], R.J. Teuscher[158,x], A. Thaler[80], O. Theiner[57], N. Themistokleous[53], T. Theveneaux-Pelzer[104], O. Thielmann[174], D.W. Thomas[97], J.P. Thomas[21], E.A. Thompson[18a], P.D. Thompson[21], E. Thomson[131], R.E. Thornberry[45], C. Tian[63a], Y. Tian[56], V. Tikhomirov[38,a], Yu.A. Tikhonov[38], S. Timoshenko[38], D. Timoshyn[136], E.X.L. Ting[1], P. Tipton[175], A. Tishelman-Charny[30], S.H. Tlou[34g], K. Todome[157], S. Todorova-Nova[136], S. Todt[51], L. Toffolin[70a,70c], M. Togawa[85], J. Tojo[90], S. Tokár[29a], K. Tokushuku[85], O. Toldaiev[69], M. Tomoto[85,113], L. Tompkins[146,m], K.W. Topolnicki[87b], E. Torrence[126], H. Torres[91], E. Torró Pastor[166], M. Toscani[31], C. Tosciri[40], M. Tost[11], D.R. Tovey[142], I.S. Trandafir[28b], T. Trefzger[169], A. Tricoli[30], I.M. Trigger[159a], S. Trincaz-Duvoid[130], D.A. Trischuk[27], B. Trocmé[61], A. Tropina[39], L. Truong[34c], M. Trzebinski[88], A. Trzupek[88], F. Tsai[148], M. Tsai[108], A. Tsiamis[155,d], P.V. Tsiareshka[38], S. Tsigaridas[159a], A. Tsirigotis[155,s], V. Tsiskaridze[158], E.G. Tskhadadze[152a], M. Tsopoulou[155], Y. Tsujikawa[89], I.I. Tsukerman[38], V. Tsulaia[18a], S. Tsuno[85], K. Tsuri[121], D. Tsybychev[148], Y. Tu[65b], A. Tudorache[28b], V. Tudorache[28b], A.N. Tuna[62], S. Turchikhin[58b,58a], I. Turk Cakir[3a], R. Turra[72a], T. Turtuvshin[39,y], P.M. Tuts[42], S. Tzamarias[155,d], E. Tzovara[102], F. Ukegawa[160], P.A. Ulloa Poblete[140c,140b], E.N. Umaka[30], G. Unal[37], A. Undrus[30], G. Unel[162], J. Urban[29b], P. Urrejola[140a], G. Usai[8], R. Ushioda[157], M. Usman[110], Z. Uysal[83], V. Vacek[135], B. Vachon[106], T. Vafeiadis[37], A. Vaitkus[98], C. Valderanis[111], E. Valdes Santurio[48a,48b], M. Valente[159a], S. Valentinetti[24b,24a], A. Valero[166], E. Valiente Moreno[166], A. Vallier[91], J.A. Valls Ferrer[166], D.R. Van Arneman[117], T.R. Van Daalen[141], A. Van Der Graaf[50], P. Van Gemmeren[6], M. Van Rijnbach[37], S. Van Stroud[98], I. Van Vulpen[117], P. Vana[136], M. Vanadia[77a,77b], W. Vandelli[37], E.R. Vandewall[124], D. Vannicola[154], L. Vannoli[54], R. Vari[76a], E.W. Varnes[7], C. Varni[18b], T. Varol[151], D. Varouchas[67], L. Varriale[166], K.E. Varvell[150], M.E. Vasile[28b], L. Vaslin[85], G.A. Vasquez[168], A. Vasyukov[39], L.M. Vaughan[124], R. Vavricka[102], T. Vazquez Schroeder[37], J. Veatch[32], V. Vecchio[103], M.J. Veen[105], I. Veliscek[30], L.M. Veloce[158], F. Veloso[133a,133c], S. Veneziano[76a], A. Ventura[71a,71b], S. Ventura Gonzalez[138], A. Verbytskyi[112], M. Verducci[75a,75b], C. Vergis[96], M. Verissimo De Araujo[84b], W. Verkerke[117], J.C. Vermeulen[117], C. Vernieri[146], M. Vessella[105], M.C. Vetterli[145,ae], A. Vgenopoulos[102], N. Viaux Maira[140f], T. Vickey[142], O.E. Vickey Boeriu[142], G.H.A. Viehhauser[129], L. Vigani[64b], M. Vigl[112], M. Villa[24b,24a], M. Villaplana Perez[166], E.M. Villhauer[53], E. Vilucchi[54], M.G. Vincter[35],

A. Visibile[117], C. Vittori[37], I. Vivarelli[24b,24a], E. Voevodina[112], F. Vogel[111], J.C. Voigt[51], P. Vokac[135], Yu. Volkotrub[87b], J. Von Ahnen[49], E. Von Toerne[25], B. Vormwald[37], V. Vorobel[136], K. Vorobev[38], M. Vos[166], K. Voss[144], M. Vozak[117], L. Vozdecky[123], N. Vranjes[16], M. Vranjes Milosavljevic[16], M. Vreeswijk[117], N.K. Vu[63d,63c], R. Vuillermet[37], O. Vujinovic[102], I. Vukotic[40], S. Wada[160], C. Wagner[105], J.M. Wagner[18a], W. Wagner[174], S. Wahdan[174], H. Wahlberg[92], J. Walder[137], R. Walker[111], W. Walkowiak[144], A. Wall[131], E.J. Wallin[100], T. Wamorkar[6], A.Z. Wang[139], C. Wang[102], C. Wang[11], H. Wang[18a], J. Wang[65c], P. Wang[98], R. Wang[62], R. Wang[6], S.M. Wang[151], S. Wang[63b], S. Wang[14], T. Wang[63a], W.T. Wang[81], W. Wang[14], X. Wang[114a], X. Wang[165], X. Wang[63c], Y. Wang[63d], Y. Wang[114a], Y. Wang[63a], Z. Wang[108], Z. Wang[63d,52,63c], Z. Wang[108], A. Warburton[106], R.J. Ward[21], N. Warrack[60], S. Waterhouse[97], A.T. Watson[21], H. Watson[60], M.F. Watson[21], E. Watton[60,137], G. Watts[141], B.M. Waugh[98], J.M. Webb[55], C. Weber[30], H.A. Weber[19], M.S. Weber[20], S.M. Weber[64a], C. Wei[63a], Y. Wei[55], A.R. Weidberg[129], E.J. Weik[120], J. Weingarten[50], C. Weiser[55], C.J. Wells[49], T. Wenaus[30], B. Wendland[50], T. Wengler[37], N.S. Wenke[112], N. Wermes[25], M. Wessels[64a], A.M. Wharton[93], A.S. White[62], A. White[8], M.J. White[1], D. Whiteson[162], L. Wickremasinghe[127], W. Wiedenmann[173], M. Wielers[137], C. Wiglesworth[43], D.J. Wilbern[123], H.G. Wilkens[37], J.J.H. Wilkinson[33], D.M. Williams[42], H.H. Williams[131], S. Williams[33], S. Willocq[105], B.J. Wilson[103], P.J. Windischhofer[40], F.I. Winkel[31], F. Winklmeier[126], B.T. Winter[55], J.K. Winter[103], M. Wittgen[146], M. Wobisch[99], T. Wojtkowski[61], Z. Wolffs[117], J. Wollrath[162], M.W. Wolter[88], H. Wolters[133a,133c], M.C. Wong[139], E.L. Woodward[42], S.D. Worm[49], B.K. Wosiek[88], K.W. Woźniak[88], S. Wozniewski[56], K. Wraight[60], C. Wu[21], M. Wu[114b], M. Wu[116], S.L. Wu[173], X. Wu[57], Y. Wu[63a], Z. Wu[4], J. Wuerzinger[112,ac], T.R. Wyatt[103], B.M. Wynne[53], S. Xella[43], L. Xia[114a], M. Xia[15], M. Xie[63a], S. Xin[14,114c], A. Xiong[126], J. Xiong[18a], D. Xu[14], H. Xu[63a], L. Xu[63a], R. Xu[131], T. Xu[108], Y. Xu[15], Z. Xu[53], Z. Xu[114a], B. Yabsley[150], S. Yacoob[34a], Y. Yamaguchi[85], E. Yamashita[156], H. Yamauchi[160], T. Yamazaki[18a], Y. Yamazaki[86], J. Yan[63c], S. Yan[60], Z. Yan[105], H.J. Yang[63c,63d], H.T. Yang[63a], S. Yang[63a], T. Yang[65c], X. Yang[37], X. Yang[14], Y. Yang[45], Y. Yang[63a], Z. Yang[63a], W-M. Yao[18a], H. Ye[114a], H. Ye[56], J. Ye[14], S. Ye[30], X. Ye[63a], Y. Yeh[98], I. Yeletskikh[39], B. Yeo[18b], M.R. Yexley[98], T.P. Yildirim[129], P. Yin[42], K. Yorita[171], S. Younas[28b], C.J.S. Young[37], C. Young[146], C. Yu[14,114c], Y. Yu[63a], J. Yuan[14,114c], M. Yuan[108], R. Yuan[63d,63c], L. Yue[98], M. Zaazoua[63a], B. Zabinski[88], E. Zaid[53], Z.K. Zak[88], T. Zakareishvili[166], S. Zambito[57], J.A. Zamora Saa[140d,140b], J. Zang[156], D. Zanzi[55], O. Zaplatilek[135], C. Zeitnitz[174], H. Zeng[14], J.C. Zeng[165], D.T. Zenger Jr[27], O. Zenin[38], T. Ženiš[29a], S. Zenz[96], S. Zerradi[36a], D. Zerwas[67], M. Zhai[14,114c], D.F. Zhang[142], J. Zhang[63b], J. Zhang[6], K. Zhang[14,114c], L. Zhang[63a], L. Zhang[114a], P. Zhang[14,114c], R. Zhang[173], S. Zhang[108], S. Zhang[91], T. Zhang[156], X. Zhang[63c], X. Zhang[63b], Y. Zhang[63c], Y. Zhang[98], Y. Zhang[114a], Z. Zhang[18a], Z. Zhang[63b], Z. Zhang[67], H. Zhao[141], T. Zhao[63b], Y. Zhao[139], Z. Zhao[63a], Z. Zhao[63a], A. Zhemchugov[39], J. Zheng[114a], K. Zheng[165], X. Zheng[63a], Z. Zheng[146], D. Zhong[165], B. Zhou[108], H. Zhou[7], N. Zhou[63c], Y. Zhou[15], Y. Zhou[114a], Y. Zhou[7], C.G. Zhu[63b], J. Zhu[108], X. Zhu[63d], Y. Zhu[63c], Y. Zhu[63a],

X. Zhuang[14], K. Zhukov[69], N.I. Zimine[39], J. Zinsser[64b], M. Ziolkowski[144], L. Živković[16], A. Zoccoli[24b,24a], K. Zoch[62], T.G. Zorbas[142], O. Zormpa[47], W. Zou[42], L. Zwalinski[37]

[1] *Department of Physics, University of Adelaide, Adelaide; Australia*
[2] *Department of Physics, University of Alberta, Edmonton AB; Canada*
[3] [(a)] *Department of Physics, Ankara University, Ankara;* [(b)] *Division of Physics, TOBB University of Economics and Technology, Ankara; Türkiye*
[4] *LAPP, Université Savoie Mont Blanc, CNRS/IN2P3, Annecy; France*
[5] *APC, Université Paris Cité, CNRS/IN2P3, Paris; France*
[6] *High Energy Physics Division, Argonne National Laboratory, Argonne IL; U.S.A.*
[7] *Department of Physics, University of Arizona, Tucson AZ; U.S.A.*
[8] *Department of Physics, University of Texas at Arlington, Arlington TX; U.S.A.*
[9] *Physics Department, National and Kapodistrian University of Athens, Athens; Greece*
[10] *Physics Department, National Technical University of Athens, Zografou; Greece*
[11] *Department of Physics, University of Texas at Austin, Austin TX; U.S.A.*
[12] *Institute of Physics, Azerbaijan Academy of Sciences, Baku; Azerbaijan*
[13] *Institut de Física d'Altes Energies (IFAE), Barcelona Institute of Science and Technology, Barcelona; Spain*
[14] *Institute of High Energy Physics, Chinese Academy of Sciences, Beijing; China*
[15] *Physics Department, Tsinghua University, Beijing; China*
[16] *Institute of Physics, University of Belgrade, Belgrade; Serbia*
[17] *Department for Physics and Technology, University of Bergen, Bergen; Norway*
[18] [(a)] *Physics Division, Lawrence Berkeley National Laboratory, Berkeley CA;* [(b)] *University of California, Berkeley CA; U.S.A.*
[19] *Institut für Physik, Humboldt Universität zu Berlin, Berlin; Germany*
[20] *Albert Einstein Center for Fundamental Physics and Laboratory for High Energy Physics, University of Bern, Bern; Switzerland*
[21] *School of Physics and Astronomy, University of Birmingham, Birmingham; U.K.*
[22] [(a)] *Department of Physics, Bogazici University, Istanbul;* [(b)] *Department of Physics Engineering, Gaziantep University, Gaziantep;* [(c)] *Department of Physics, Istanbul University, Istanbul; Türkiye*
[23] [(a)] *Facultad de Ciencias y Centro de Investigaciónes, Universidad Antonio Nariño, Bogotá;* [(b)] *Departamento de Física, Universidad Nacional de Colombia, Bogotá; Colombia*
[24] [(a)] *Dipartimento di Fisica e Astronomia A. Righi, Università di Bologna, Bologna;* [(b)] *INFN Sezione di Bologna; Italy*
[25] *Physikalisches Institut, Universität Bonn, Bonn; Germany*
[26] *Department of Physics, Boston University, Boston MA; U.S.A.*
[27] *Department of Physics, Brandeis University, Waltham MA; U.S.A.*
[28] [(a)] *Transilvania University of Brasov, Brasov;* [(b)] *Horia Hulubei National Institute of Physics and Nuclear Engineering, Bucharest;* [(c)] *Department of Physics, Alexandru Ioan Cuza University of Iasi, Iasi;* [(d)] *National Institute for Research and Development of Isotopic and Molecular Technologies, Physics Department, Cluj-Napoca;* [(e)] *National University of Science and Technology Politechnica, Bucharest;* [(f)] *West University in Timisoara, Timisoara;* [(g)] *Faculty of Physics, University of Bucharest, Bucharest; Romania*
[29] [(a)] *Faculty of Mathematics, Physics and Informatics, Comenius University, Bratislava;* [(b)] *Department of Subnuclear Physics, Institute of Experimental Physics of the Slovak Academy of Sciences, Kosice; Slovak Republic*
[30] *Physics Department, Brookhaven National Laboratory, Upton NY; U.S.A.*
[31] *Universidad de Buenos Aires, Facultad de Ciencias Exactas y Naturales, Departamento de Física, y CONICET, Instituto de Física de Buenos Aires (IFIBA), Buenos Aires; Argentina*
[32] *California State University, CA; U.S.A.*
[33] *Cavendish Laboratory, University of Cambridge, Cambridge; U.K.*
[34] [(a)] *Department of Physics, University of Cape Town, Cape Town;* [(b)] *iThemba Labs, Western Cape;* [(c)] *Department of Mechanical Engineering Science, University of Johannesburg, Johannesburg;* [(d)] *National Institute of Physics, University of the Philippines Diliman*

JHEP10(2024)104

(Philippines);[e] *University of South Africa, Department of Physics, Pretoria;*[f] *University of Zululand, KwaDlangezwa;*[g] *School of Physics, University of the Witwatersrand, Johannesburg; South Africa*
[35] *Department of Physics, Carleton University, Ottawa ON; Canada*
[36] [a] *Faculté des Sciences Ain Chock, Université Hassan II de Casablanca;*[b] *Faculté des Sciences, Université Ibn-Tofail, Kénitra;*[c] *Faculté des Sciences Semlalia, Université Cadi Ayyad, LPHEA-Marrakech;*[d] *LPMR, Faculté des Sciences, Université Mohamed Premier, Oujda;*[e] *Faculté des sciences, Université Mohammed V, Rabat;*[f] *Institute of Applied Physics, Mohammed VI Polytechnic University, Ben Guerir; Morocco*
[37] *CERN, Geneva; Switzerland*
[38] *Affiliated with an institute covered by a cooperation agreement with CERN*
[39] *Affiliated with an international laboratory covered by a cooperation agreement with CERN*
[40] *Enrico Fermi Institute, University of Chicago, Chicago IL; U.S.A.*
[41] *LPC, Université Clermont Auvergne, CNRS/IN2P3, Clermont-Ferrand; France*
[42] *Nevis Laboratory, Columbia University, Irvington NY; U.S.A.*
[43] *Niels Bohr Institute, University of Copenhagen, Copenhagen; Denmark*
[44] [a] *Dipartimento di Fisica, Università della Calabria, Rende;*[b] *INFN Gruppo Collegato di Cosenza, Laboratori Nazionali di Frascati; Italy*
[45] *Physics Department, Southern Methodist University, Dallas TX; U.S.A.*
[46] *Physics Department, University of Texas at Dallas, Richardson TX; U.S.A.*
[47] *National Centre for Scientific Research "Demokritos", Agia Paraskevi; Greece*
[48] [a] *Department of Physics, Stockholm University;*[b] *Oskar Klein Centre, Stockholm; Sweden*
[49] *Deutsches Elektronen-Synchrotron DESY, Hamburg and Zeuthen; Germany*
[50] *Fakultät Physik , Technische Universität Dortmund, Dortmund; Germany*
[51] *Institut für Kern- und Teilchenphysik, Technische Universität Dresden, Dresden; Germany*
[52] *Department of Physics, Duke University, Durham NC; U.S.A.*
[53] *SUPA - School of Physics and Astronomy, University of Edinburgh, Edinburgh; U.K.*
[54] *INFN e Laboratori Nazionali di Frascati, Frascati; Italy*
[55] *Physikalisches Institut, Albert-Ludwigs-Universität Freiburg, Freiburg; Germany*
[56] *II. Physikalisches Institut, Georg-August-Universität Göttingen, Göttingen; Germany*
[57] *Département de Physique Nucléaire et Corpusculaire, Université de Genève, Genève; Switzerland*
[58] [a] *Dipartimento di Fisica, Università di Genova, Genova;*[b] *INFN Sezione di Genova; Italy*
[59] *II. Physikalisches Institut, Justus-Liebig-Universität Giessen, Giessen; Germany*
[60] *SUPA - School of Physics and Astronomy, University of Glasgow, Glasgow; U.K.*
[61] *LPSC, Université Grenoble Alpes, CNRS/IN2P3, Grenoble INP, Grenoble; France*
[62] *Laboratory for Particle Physics and Cosmology, Harvard University, Cambridge MA; U.S.A.*
[63] [a] *Department of Modern Physics and State Key Laboratory of Particle Detection and Electronics, University of Science and Technology of China, Hefei;*[b] *Institute of Frontier and Interdisciplinary Science and Key Laboratory of Particle Physics and Particle Irradiation (MOE), Shandong University, Qingdao;*[c] *School of Physics and Astronomy, Shanghai Jiao Tong University, Key Laboratory for Particle Astrophysics and Cosmology (MOE), SKLPPC, Shanghai;*[d] *Tsung-Dao Lee Institute, Shanghai;*[e] *School of Physics and Microelectronics, Zhengzhou University; China*
[64] [a] *Kirchhoff-Institut für Physik, Ruprecht-Karls-Universität Heidelberg, Heidelberg;*[b] *Physikalisches Institut, Ruprecht-Karls-Universität Heidelberg, Heidelberg; Germany*
[65] [a] *Department of Physics, Chinese University of Hong Kong, Shatin, N.T., Hong Kong;*[b] *Department of Physics, University of Hong Kong, Hong Kong;*[c] *Department of Physics and Institute for Advanced Study, Hong Kong University of Science and Technology, Clear Water Bay, Kowloon, Hong Kong; China*
[66] *Department of Physics, National Tsing Hua University, Hsinchu; Taiwan*
[67] *IJCLab, Université Paris-Saclay, CNRS/IN2P3, 91405, Orsay; France*
[68] *Centro Nacional de Microelectrónica (IMB-CNM-CSIC), Barcelona; Spain*
[69] *Department of Physics, Indiana University, Bloomington IN; U.S.A.*
[70] [a] *INFN Gruppo Collegato di Udine, Sezione di Trieste, Udine;*[b] *ICTP, Trieste;*[c] *Dipartimento Politecnico di Ingegneria e Architettura, Università di Udine, Udine; Italy*
[71] [a] *INFN Sezione di Lecce;*[b] *Dipartimento di Matematica e Fisica, Università del Salento, Lecce; Italy*
[72] [a] *INFN Sezione di Milano;*[b] *Dipartimento di Fisica, Università di Milano, Milano; Italy*

[73] [(a)] *INFN Sezione di Napoli;*[(b)] *Dipartimento di Fisica, Università di Napoli, Napoli; Italy*
[74] [(a)] *INFN Sezione di Pavia;*[(b)] *Dipartimento di Fisica, Università di Pavia, Pavia; Italy*
[75] [(a)] *INFN Sezione di Pisa;*[(b)] *Dipartimento di Fisica E. Fermi, Università di Pisa, Pisa; Italy*
[76] [(a)] *INFN Sezione di Roma;*[(b)] *Dipartimento di Fisica, Sapienza Università di Roma, Roma; Italy*
[77] [(a)] *INFN Sezione di Roma Tor Vergata;*[(b)] *Dipartimento di Fisica, Università di Roma Tor Vergata, Roma; Italy*
[78] [(a)] *INFN Sezione di Roma Tre;*[(b)] *Dipartimento di Matematica e Fisica, Università Roma Tre, Roma; Italy*
[79] [(a)] *INFN-TIFPA;*[(b)] *Università degli Studi di Trento, Trento; Italy*
[80] *Universität Innsbruck, Department of Astro and Particle Physics, Innsbruck; Austria*
[81] *University of Iowa, Iowa City IA; U.S.A.*
[82] *Department of Physics and Astronomy, Iowa State University, Ames IA; U.S.A.*
[83] *Istinye University, Sariyer, Istanbul; Türkiye*
[84] [(a)] *Departamento de Engenharia Elétrica, Universidade Federal de Juiz de Fora (UFJF), Juiz de Fora;*[(b)] *Universidade Federal do Rio De Janeiro COPPE/EE/IF, Rio de Janeiro;*[(c)] *Instituto de Física, Universidade de São Paulo, São Paulo;*[(d)] *Rio de Janeiro State University, Rio de Janeiro;*[(e)] *Federal University of Bahia, Bahia; Brazil*
[85] *KEK, High Energy Accelerator Research Organization, Tsukuba; Japan*
[86] *Graduate School of Science, Kobe University, Kobe; Japan*
[87] [(a)] *AGH University of Krakow, Faculty of Physics and Applied Computer Science, Krakow;*[(b)] *Marian Smoluchowski Institute of Physics, Jagiellonian University, Krakow; Poland*
[88] *Institute of Nuclear Physics Polish Academy of Sciences, Krakow; Poland*
[89] *Faculty of Science, Kyoto University, Kyoto; Japan*
[90] *Research Center for Advanced Particle Physics and Department of Physics, Kyushu University, Fukuoka; Japan*
[91] *L2IT, Université de Toulouse, CNRS/IN2P3, UPS, Toulouse; France*
[92] *Instituto de Física La Plata, Universidad Nacional de La Plata and CONICET, La Plata; Argentina*
[93] *Physics Department, Lancaster University, Lancaster; U.K.*
[94] *Oliver Lodge Laboratory, University of Liverpool, Liverpool; U.K.*
[95] *Department of Experimental Particle Physics, Jožef Stefan Institute and Department of Physics, University of Ljubljana, Ljubljana; Slovenia*
[96] *School of Physics and Astronomy, Queen Mary University of London, London; U.K.*
[97] *Department of Physics, Royal Holloway University of London, Egham; U.K.*
[98] *Department of Physics and Astronomy, University College London, London; U.K.*
[99] *Louisiana Tech University, Ruston LA; U.S.A.*
[100] *Fysiska institutionen, Lunds universitet, Lund; Sweden*
[101] *Departamento de Física Teorica C-15 and CIAFF, Universidad Autónoma de Madrid, Madrid; Spain*
[102] *Institut für Physik, Universität Mainz, Mainz; Germany*
[103] *School of Physics and Astronomy, University of Manchester, Manchester; U.K.*
[104] *CPPM, Aix-Marseille Université, CNRS/IN2P3, Marseille; France*
[105] *Department of Physics, University of Massachusetts, Amherst MA; U.S.A.*
[106] *Department of Physics, McGill University, Montreal QC; Canada*
[107] *School of Physics, University of Melbourne, Victoria; Australia*
[108] *Department of Physics, University of Michigan, Ann Arbor MI; U.S.A.*
[109] *Department of Physics and Astronomy, Michigan State University, East Lansing MI; U.S.A.*
[110] *Group of Particle Physics, University of Montreal, Montreal QC; Canada*
[111] *Fakultät für Physik, Ludwig-Maximilians-Universität München, München; Germany*
[112] *Max-Planck-Institut für Physik (Werner-Heisenberg-Institut), München; Germany*
[113] *Graduate School of Science and Kobayashi-Maskawa Institute, Nagoya University, Nagoya; Japan*
[114] [(a)] *Department of Physics, Nanjing University, Nanjing;*[(b)] *School of Science, Shenzhen Campus of Sun Yat-sen University;*[(c)] *University of Chinese Academy of Science (UCAS), Beijing; China*
[115] *Department of Physics and Astronomy, University of New Mexico, Albuquerque NM; U.S.A.*
[116] *Institute for Mathematics, Astrophysics and Particle Physics, Radboud University/Nikhef, Nijmegen; Netherlands*

JHEP10(2024)104

[117] *Nikhef National Institute for Subatomic Physics and University of Amsterdam, Amsterdam; Netherlands*
[118] *Department of Physics, Northern Illinois University, DeKalb IL; U.S.A.*
[119] [(a)] *New York University Abu Dhabi, Abu Dhabi;* [(b)] *United Arab Emirates University, Al Ain; United Arab Emirates*
[120] *Department of Physics, New York University, New York NY; U.S.A.*
[121] *Ochanomizu University, Otsuka, Bunkyo-ku, Tokyo; Japan*
[122] *Ohio State University, Columbus OH; U.S.A.*
[123] *Homer L. Dodge Department of Physics and Astronomy, University of Oklahoma, Norman OK; U.S.A.*
[124] *Department of Physics, Oklahoma State University, Stillwater OK; U.S.A.*
[125] *Palacký University, Joint Laboratory of Optics, Olomouc; Czech Republic*
[126] *Institute for Fundamental Science, University of Oregon, Eugene, OR; U.S.A.*
[127] *Graduate School of Science, Osaka University, Osaka; Japan*
[128] *Department of Physics, University of Oslo, Oslo; Norway*
[129] *Department of Physics, Oxford University, Oxford; U.K.*
[130] *LPNHE, Sorbonne Université, Université Paris Cité, CNRS/IN2P3, Paris; France*
[131] *Department of Physics, University of Pennsylvania, Philadelphia PA; U.S.A.*
[132] *Department of Physics and Astronomy, University of Pittsburgh, Pittsburgh PA; U.S.A.*
[133] [(a)] *Laboratório de Instrumentação e Física Experimental de Partículas - LIP, Lisboa;* [(b)] *Departamento de Física, Faculdade de Ciências, Universidade de Lisboa, Lisboa;* [(c)] *Departamento de Física, Universidade de Coimbra, Coimbra;* [(d)] *Centro de Física Nuclear da Universidade de Lisboa, Lisboa;* [(e)] *Departamento de Física, Universidade do Minho, Braga;* [(f)] *Departamento de Física Teórica y del Cosmos, Universidad de Granada, Granada (Spain);* [(g)] *Departamento de Física, Instituto Superior Técnico, Universidade de Lisboa, Lisboa; Portugal*
[134] *Institute of Physics of the Czech Academy of Sciences, Prague; Czech Republic*
[135] *Czech Technical University in Prague, Prague; Czech Republic*
[136] *Charles University, Faculty of Mathematics and Physics, Prague; Czech Republic*
[137] *Particle Physics Department, Rutherford Appleton Laboratory, Didcot; U.K.*
[138] *IRFU, CEA, Université Paris-Saclay, Gif-sur-Yvette; France*
[139] *Santa Cruz Institute for Particle Physics, University of California Santa Cruz, Santa Cruz CA; U.S.A.*
[140] [(a)] *Departamento de Física, Pontificia Universidad Católica de Chile, Santiago;* [(b)] *Millennium Institute for Subatomic physics at high energy frontier (SAPHIR), Santiago;* [(c)] *Instituto de Investigación Multidisciplinario en Ciencia y Tecnología, y Departamento de Física, Universidad de La Serena;* [(d)] *Universidad Andres Bello, Department of Physics, Santiago;* [(e)] *Instituto de Alta Investigación, Universidad de Tarapacá, Arica;* [(f)] *Departamento de Física, Universidad Técnica Federico Santa María, Valparaíso; Chile*
[141] *Department of Physics, University of Washington, Seattle WA; U.S.A.*
[142] *Department of Physics and Astronomy, University of Sheffield, Sheffield; U.K.*
[143] *Department of Physics, Shinshu University, Nagano; Japan*
[144] *Department Physik, Universität Siegen, Siegen; Germany*
[145] *Department of Physics, Simon Fraser University, Burnaby BC; Canada*
[146] *SLAC National Accelerator Laboratory, Stanford CA; U.S.A.*
[147] *Department of Physics, Royal Institute of Technology, Stockholm; Sweden*
[148] *Departments of Physics and Astronomy, Stony Brook University, Stony Brook NY; U.S.A.*
[149] *Department of Physics and Astronomy, University of Sussex, Brighton; U.K.*
[150] *School of Physics, University of Sydney, Sydney; Australia*
[151] *Institute of Physics, Academia Sinica, Taipei; Taiwan*
[152] [(a)] *E. Andronikashvili Institute of Physics, Iv. Javakhishvili Tbilisi State University, Tbilisi;* [(b)] *High Energy Physics Institute, Tbilisi State University, Tbilisi;* [(c)] *University of Georgia, Tbilisi; Georgia*
[153] *Department of Physics, Technion, Israel Institute of Technology, Haifa; Israel*
[154] *Raymond and Beverly Sackler School of Physics and Astronomy, Tel Aviv University, Tel Aviv; Israel*
[155] *Department of Physics, Aristotle University of Thessaloniki, Thessaloniki; Greece*
[156] *International Center for Elementary Particle Physics and Department of Physics, University of Tokyo, Tokyo; Japan*

JHEP10(2024)104

[157] *Department of Physics, Tokyo Institute of Technology, Tokyo; Japan*
[158] *Department of Physics, University of Toronto, Toronto ON; Canada*
[159] [(a)] *TRIUMF, Vancouver BC;*[(b)] *Department of Physics and Astronomy, York University, Toronto ON; Canada*
[160] *Division of Physics and Tomonaga Center for the History of the Universe, Faculty of Pure and Applied Sciences, University of Tsukuba, Tsukuba; Japan*
[161] *Department of Physics and Astronomy, Tufts University, Medford MA; U.S.A.*
[162] *Department of Physics and Astronomy, University of California Irvine, Irvine CA; U.S.A.*
[163] *University of Sharjah, Sharjah; United Arab Emirates*
[164] *Department of Physics and Astronomy, University of Uppsala, Uppsala; Sweden*
[165] *Department of Physics, University of Illinois, Urbana IL; U.S.A.*
[166] *Instituto de Física Corpuscular (IFIC), Centro Mixto Universidad de Valencia - CSIC, Valencia; Spain*
[167] *Department of Physics, University of British Columbia, Vancouver BC; Canada*
[168] *Department of Physics and Astronomy, University of Victoria, Victoria BC; Canada*
[169] *Fakultät für Physik und Astronomie, Julius-Maximilians-Universität Würzburg, Würzburg; Germany*
[170] *Department of Physics, University of Warwick, Coventry; U.K.*
[171] *Waseda University, Tokyo; Japan*
[172] *Department of Particle Physics and Astrophysics, Weizmann Institute of Science, Rehovot; Israel*
[173] *Department of Physics, University of Wisconsin, Madison WI; U.S.A.*
[174] *Fakultät für Mathematik und Naturwissenschaften, Fachgruppe Physik, Bergische Universität Wuppertal, Wuppertal; Germany*
[175] *Department of Physics, Yale University, New Haven CT; U.S.A.*

[a] *Also Affiliated with an institute covered by a cooperation agreement with CERN*
[b] *Also at An-Najah National University, Nablus; Palestine*
[c] *Also at Borough of Manhattan Community College, City University of New York, New York NY; U.S.A.*
[d] *Also at Center for Interdisciplinary Research and Innovation (CIRI-AUTH), Thessaloniki; Greece*
[e] *Also at Centro Studi e Ricerche Enrico Fermi; Italy*
[f] *Also at CERN, Geneva; Switzerland*
[g] *Also at CMD-AC UNEC Research Center, Azerbaijan State University of Economics (UNEC); Azerbaijan*
[h] *Also at Département de Physique Nucléaire et Corpusculaire, Université de Genève, Genève; Switzerland*
[i] *Also at Departament de Fisica de la Universitat Autonoma de Barcelona, Barcelona; Spain*
[j] *Also at Department of Financial and Management Engineering, University of the Aegean, Chios; Greece*
[k] *Also at Department of Physics, California State University, Sacramento; U.S.A.*
[l] *Also at Department of Physics, King's College London, London; U.K.*
[m] *Also at Department of Physics, Stanford University, Stanford CA; U.S.A.*
[n] *Also at Department of Physics, Stellenbosch University; South Africa*
[o] *Also at Department of Physics, University of Fribourg, Fribourg; Switzerland*
[p] *Also at Department of Physics, University of Thessaly; Greece*
[q] *Also at Department of Physics, Westmont College, Santa Barbara; U.S.A.*
[r] *Also at Faculty of Physics, Sofia University, 'St. Kliment Ohridski', Sofia; Bulgaria*
[s] *Also at Hellenic Open University, Patras; Greece*
[t] *Also at Institucio Catalana de Recerca i Estudis Avancats, ICREA, Barcelona; Spain*
[u] *Also at Institut für Experimentalphysik, Universität Hamburg, Hamburg; Germany*
[v] *Also at Institute for Nuclear Research and Nuclear Energy (INRNE) of the Bulgarian Academy of Sciences, Sofia; Bulgaria*
[w] *Also at Institute of Applied Physics, Mohammed VI Polytechnic University, Ben Guerir; Morocco*
[x] *Also at Institute of Particle Physics (IPP); Canada*
[y] *Also at Institute of Physics and Technology, Mongolian Academy of Sciences, Ulaanbaatar; Mongolia*
[z] *Also at Institute of Physics, Azerbaijan Academy of Sciences, Baku; Azerbaijan*
[aa] *Also at Institute of Theoretical Physics, Ilia State University, Tbilisi; Georgia*
[ab] *Also at National Institute of Physics, University of the Philippines Diliman (Philippines); Philippines*
[ac] *Also at Technical University of Munich, Munich; Germany*
[ad] *Also at The Collaborative Innovation Center of Quantum Matter (CICQM), Beijing; China*

[ae] *Also at TRIUMF, Vancouver BC; Canada*
[af] *Also at Università di Napoli Parthenope, Napoli; Italy*
[ag] *Also at University of Colorado Boulder, Department of Physics, Colorado; U.S.A.*
[ah] *Also at Washington College, Chestertown, MD; U.S.A.*
[ai] *Also at Yeditepe University, Physics Department, Istanbul; Türkiye*
[*] *Deceased*

JHEP10(2024)104